TECHNICAL UNIVERSITY- GABROVO

Faculty of Mechanical and Precision Engineering

Eng. Petya Hristoforova Daskalova, MSc

Increasing the fatigue life of fastener holes in aluminum alloy D 16 AT using a modified split mandrel cold working method

AUTHOR's ABSTRACT

of a Dissertation for acquiring the educational and scientific degree "Doctor" (PhD)

Field of higher education: 5. Technical sciences

Professional field: 5.1. Mechanical engineering

Doctoral program: Construction Mechanics, Strength of Materials

Research supervisors: Prof. Eng. Jordan Todorov Maximov, DSc
Prof. Eng. Galya Velikova Duncheva, DSc

Reviewers: Prof. Eng. Nikolay Dimitrov Minchev, DSc
Prof. Eng. Stoyko Atanasov Gyurov, PhD

Gabrovo, 2025

The dissertation work was discussed and scheduled for official defense at a meeting of the Extended Department Council of the Department of Mechanical Engineering and Technologies at the Faculty of Mechanical Engineering and Instrumentation of the Technical University - Gabrovo, held on 12th December 2025.

The dissertation consists of: Contents, Accepted symbols and abbreviations, Introduction, 4 chapters, Classification of contributions, Article publications and used total literature of 95 pages, which include text, formulas, 46 figures and graphics and 4 tables. The literature covers 128 titles, papers, reports, books and internet sites.

The development of the dissertation was carried out in the Department of Mechanical Engineering and Technologies at the Faculty of Mechanical Engineering and Instrumentation of the Technical University - Gabrovo, Technological Park of Technical University – Gabrovo.

The official defense of the dissertation will take place on 03.04.2026 at 13:30 in the Conference Hall of the Technical University - Gabrovo.

Autor: Petya Hristoforova Daskalova

Title: Increasing the fatigue life of fastener holes in aluminum alloy D 16 AT using a modified split mandrel cold working method
Edition: 20
Place of print:
“Vasil Aprilov” publishers of Technical university - Gabrovo

ACCEPTED ABBREVIATIONS

***CNC** – Computer numerical control*
***DCE** – Degree of cold expansion*
***FEM** – Finite element method*
***IF** – Interference fitting*
***LSP** – Laser shock peening*
***MSMCW** – Modified Split Mandrel Cold Working*
***SEM** – Scanning Electron Microscope*
***SI** – Surface integrity*
***SMCW** – Split Mandrel Cold Working*
***SP** – Shot peening*
***SSCE** – Split Sleeve Cold Expansion*
***DB** – Diamand Burnishing*
***DCEx** – Direct cold expansion*
***FE** – Finite element*
***RSs** – residual stresses*
***SCW** – Surface Cold Working*
***FH** – Fastener holes*
***CEHM** – Cold expansion of holes method*
***SCE** – Symmetric cold expansion*
***FL** – Fatigue life*

ACCEPTED SYMBOLS

Latin

A_5 *– Elongation*
***D** – Circumscribed diameter of the tool's forming section*
d_0 *– Pre-machined hole diameter*
d_t *– Mandrel major diameter*
E *– Young Modulus*
F_b *– Deforming force*
***f** – Feed rate*
***J** – Axial moment of inertia of the elastic beam's cross-section*
***i** – Nominal tightness*
***l** – Length of the elastic beam*
***N** – Number of cycles to fatigue failure*
n_s *– Number of segments of the tool's working part*
$R_{0.2}$ *– Yield strength*
R_a *– (Average roughness) measures the deviation of a surface from a mean height*
R_m *– Tensile strength*
R_z *– Roughness parameter which measures the difference between the highest peak and lowest valley*
***t** – Thickness of the bushing*

Greek

$\boldsymbol{\sigma_t^{res}}$ – *Hoop compressive residual stresses*
$\boldsymbol{\varepsilon_{t,0}}$ – *Hoop strain of the points of the hole surface*
$\boldsymbol{\omega_e}$ – *Angular velocity around the hole axis*
$\boldsymbol{\omega_r}$ – *Angular velocity around its own axis*
$\boldsymbol{\delta}$ – *Thickness of the cut of the tool's working part*
$\boldsymbol{\Delta}$ – *Deflection*
$\boldsymbol{\sigma_a}$ – *Normal stress amplitude*
$\boldsymbol{\theta}$ – *Nutation angle*

OVERWIE OF THE DISSERTATION PAPER

Relevance of the problem

High-strength aluminum alloys are wildly use in aircraft industry, because of their favorable strength /weight ratio. They are preferably used in production of aircraft skins, panels, frames, beams and another critical structural parts in aircraft construction. The assembly of these parts is done by fastener holes (FH). Typical representative of these materials is aluminum alloy 2024-T3, which is analog of D 16 AT. FH are natural concentrators of stress and strains. Dynamic stresses during use cause material fatigue, which starts around of the surface of the FH. A proven effective way of fatigue life of aluminum components of FH is their cold expansion. The concept of cold expansion of the FH is developed and patented for use in the aircraft industry by Boeing company. The main idea of this concept is the creation of sufficiently intensive zone of residual hoop stresses the hole, which similar to a bracket slows down the development of dangerous fatigue cracks of I-st type- rupture cracks increasing significantly fatigue life and secure use.

The cold expansion of holes method (CEH) through a deforming passing along the axes of hole with tightness is widely used in practice. The most commonly used methods are Split Sleeve Cold Expansion (SSCE) and Split Mandrel Cold Working (SMCW). Both methods require technological cycles containing wide number of control operations combined with a narrow tolerance of the size of preprocessed FH. To overcome this shortcoming a modified version of the Split Mandrel Cold Working (MSMCW) method provides constant tightness with relatively wide tolerance of the initial diameter of the hole. As a result, the technological cycle for CE is reduced, which significantly reduces the time and total production coast.

Dissertation paper is aimed at evaluating the effectiveness of MSMCW in improving surface integrity (SI) characteristics around the holes in correlation with the fatigue behavior of pulsating tensile of the workpiece aluminum alloy 2024-T3. The obtained experimental results correspond to the worst sceneries of dispersion of the diameters of the pre-drilled FH, i.e. all experimental studies were caried out under conditions of excessively large dispersion compared to the usual engineering practice of the diameters of the treated FH.

Aims and tasks of the thesis

The main objective of the thesis is to experimentally determine the effectiveness of the new Modified Split Mandrel Cold Working (MSMCW) *method for improving SI of CEH and increasing the FL of structural elements made of aluminum alloy 2024-T3 under conditions of a relatively large tolerance of the pre-machined holes.*

The following main objectives were accomplished to reach the aim:

1). *The main approaches and the modern methods/techniques for increasing for the FL of structural elements with FH were systematized and analyzed;*

2). The parameters of the tool and device for MSMCW implementation were evaluated;

3). *The characteristics of SI of the material around the CEH were investigated in terms of the distribution of RSs, microhardness and microstructure in bush-type workpiece subjected to cold expansion using MSMCW under conditions of a relatively large tolerance of the pre-drilled holes;*

4). A comparative experimental study of the fatigue behavior of flat fatigue workpiece with FH, from aluminum alloy 2024-T3 subjected to cold expansion using MSMCW under conditions of a relatively large tolerance of the pre-drilled holes was conducted.

Methods of study

A series of experimental studies on workpiece of aluminum alloy 2024-T3, which is analog of D16T, which include: microstructural analysis through optical microscopy and SEM, studies of the profiles of microhardness in depth of surface of the holes, x-ray diffraction analysis assessment hoop RSs, fatigue tests, pulsating tension of flat workpiece with holes are conducted.

The author defends the thesis

♦ Morphological classification scheme basic approaches and implementing them methods for increasing FL of metal constructional elements with FH;

♦ The effectiveness of the MSMCW method for insuring on intensive and deep zone beneficial comparative hoop residual stresses in bush-type workpiece of aluminum alloy 2024-T3 in conditions of excessively large scattering of the diameters of the pre-drilled holes.;

♦ The effectiveness of the MSMCW method for hardening and modified the material around CEH in aluminum alloy 2024-T3 ;

♦ The beneficial effect of homogenization of RSs in axial direction using removal of surface cold worked layer with suitable thickness around the holes in the final reaming for increasing of the FL of the pulsating cycle of aluminum alloy 2024-T3;

♦ $S - N$ curves fatigue behavior in a pulsating cycle prove the effectiveness of the MSMCW method in conditions of excessively large scattering of the pre-drilled hole diameters for increasing FL of aluminum alloy 2024-T3 more than 6^{th} times (on a basic of 10^6 cycle fatigue strength cycle) in comparison with conventional process of holes only with drilling.

Practical use

The MSMCW method provides intensive a deep zone implemented beneficial compressive hoop RSs and modifies the material around FH in conditions of large admissions of diameters of pre-drilled holes, which lead to significant of FL. Therefore, the utilization of the MSMCW method in conditions of the usual for the engineering praxis admissions of the diameters of the pre-drilled holes will reduce the scattering of the SI around CEH. In result the fatigue behavior of components with FH of aluminum alloys will significantly improve which provides more beneficial price/quality ratio.

Work approbation

The dissertation paper is reported and discussed extended department meeting of "Material science and mechanics of materials" at Technical University of Gabrovo. Stages of the dissertation work are published in international magazine "Metals" (IF 2.5), magazine "Journal of the Technical University of Gabrovo".

Publishing

On the thesis of the dissertation work are published one article in the international magazine "Metals", national magazine of the national reference list (magazine "Journal of the Technical University of Gabrovo) and three science reports in international science conference on science reviewing.

Content of dissertation paper

Chapter 1. MODERN VIEW OF THE INCREASING OF THE FATIGUE LIFE OF STRUCTURAL ELEMENTS WITH FASTENER HOLES PROBLEM

1.2. A generalized classification scheme of methods for increasing the fatigue life of structural elements with fastener holes

General approach of introducing pressure RSs in metal structural elements is the mechanical treatment through mechanical cold working. On that base in dissertation paper is suggested s generalized classification scheme of the methods for increasing FL of metal structural elements with FH (fig. 1.7).

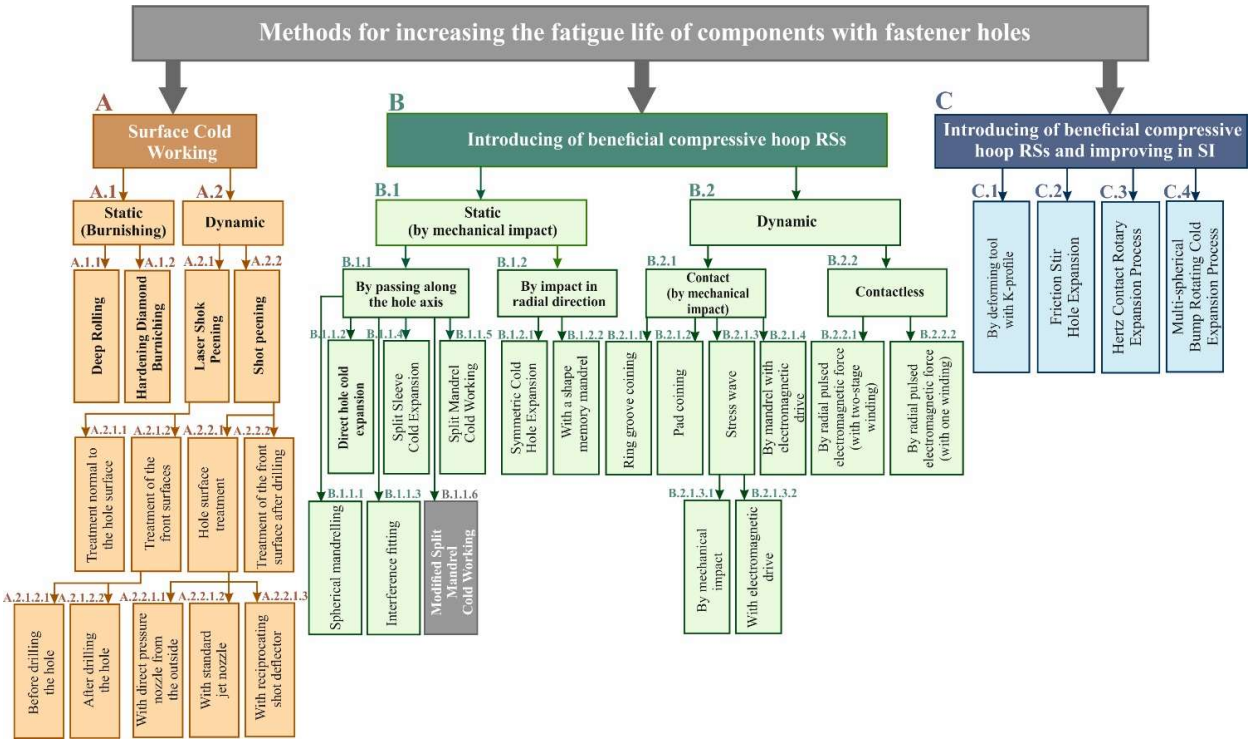

Fig. 1.7. A generalized classification scheme of the methods for increasing the fatigue life of structural elements with fastener holes

Subject systematization are the established methods in engineering practice and new methods for treating of holes developed in recent years. Generalized classification scheme is developed on the bases of the differential – morphological method using hierarchical sign and sub – signs. Each element is uniquely identified with a corresponding letter or letter – numerical cold in accordance with the hierarchical level of the used morphological signs and sub – sings. In the generalized classification scheme (Fig. 1. 7.) for main classification signs at the first level, the main approaches for modifying the material around fastener holes are adopted, indicated as follows:

- A – Surface cold working;
- B – Introducing of beneficial compressive hoop RSs;
- C – Introducing of beneficial compressive hoop RSs and improving in SI.

At the next hierarchical levels in the generalized classification scheme, for each of the main approaches, classification of the methods implementing them is made, for this purpose, their defining characteristics, accepted as sub-characteristics, were selected.

1.3. Analysis of modern methods for increasing the FL of structural elements with FH

1.3.1. Method for Surface Cold Working

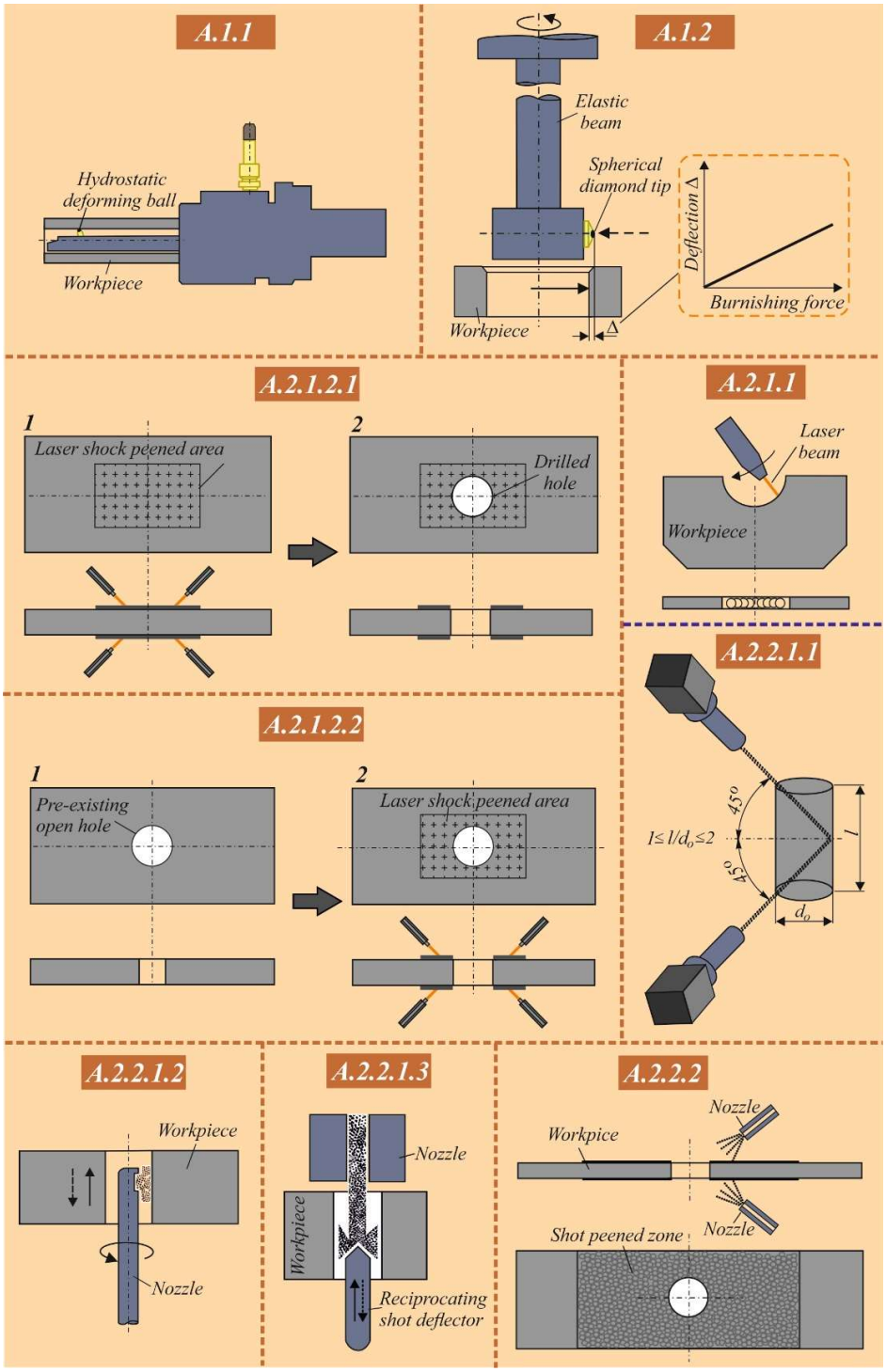

Fig. 1.8 Principal schemes of the methods based on surface cold working

Principal schemes of the most commonly used static methods (Group A.1) and dynamic methods (Group A. 2) surface cold working (SCW) of holes are displayed on fig. 1.8. Designation of the methods corresponds to the accepted symbols in the generalized classification scheme (fig. 1.7).

1.3.2. Methods for introducing beneficial hoop compressive RSs

1.3.2.1. Static methods (group B.1)

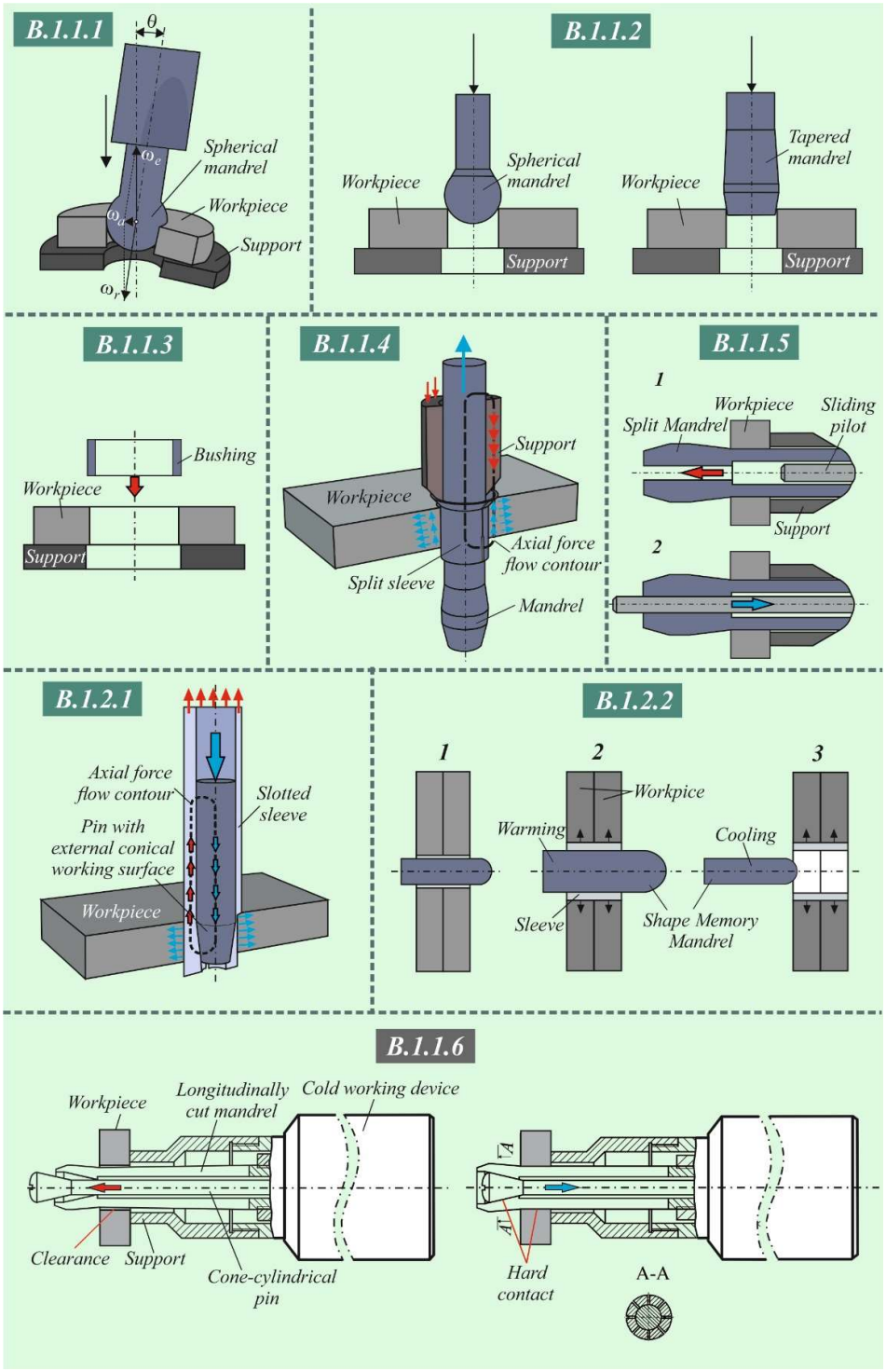

Fig. 1.9 Principal schemes of the static methods for introducing beneficial compressive RSs

Principal schemes of the most commonly used static methods are visualized on fig. 1.9, and designations correspond with these on the fig. 1.7.

1.3.2.2. Dynamic methods (group B.2)

Principle schemes of the dynamic methods for introducing beneficial compressive RSs are shown to fig. 1.10. According to the way of applying the dynamic impact, the methods of group B.2 are (fig.

1.7): 1). Contact (by mechanical impact) (subgroup B.2.1) and 2). Non-contact (by radial pulsating electromagnetic force) (subgroup B.2.2).

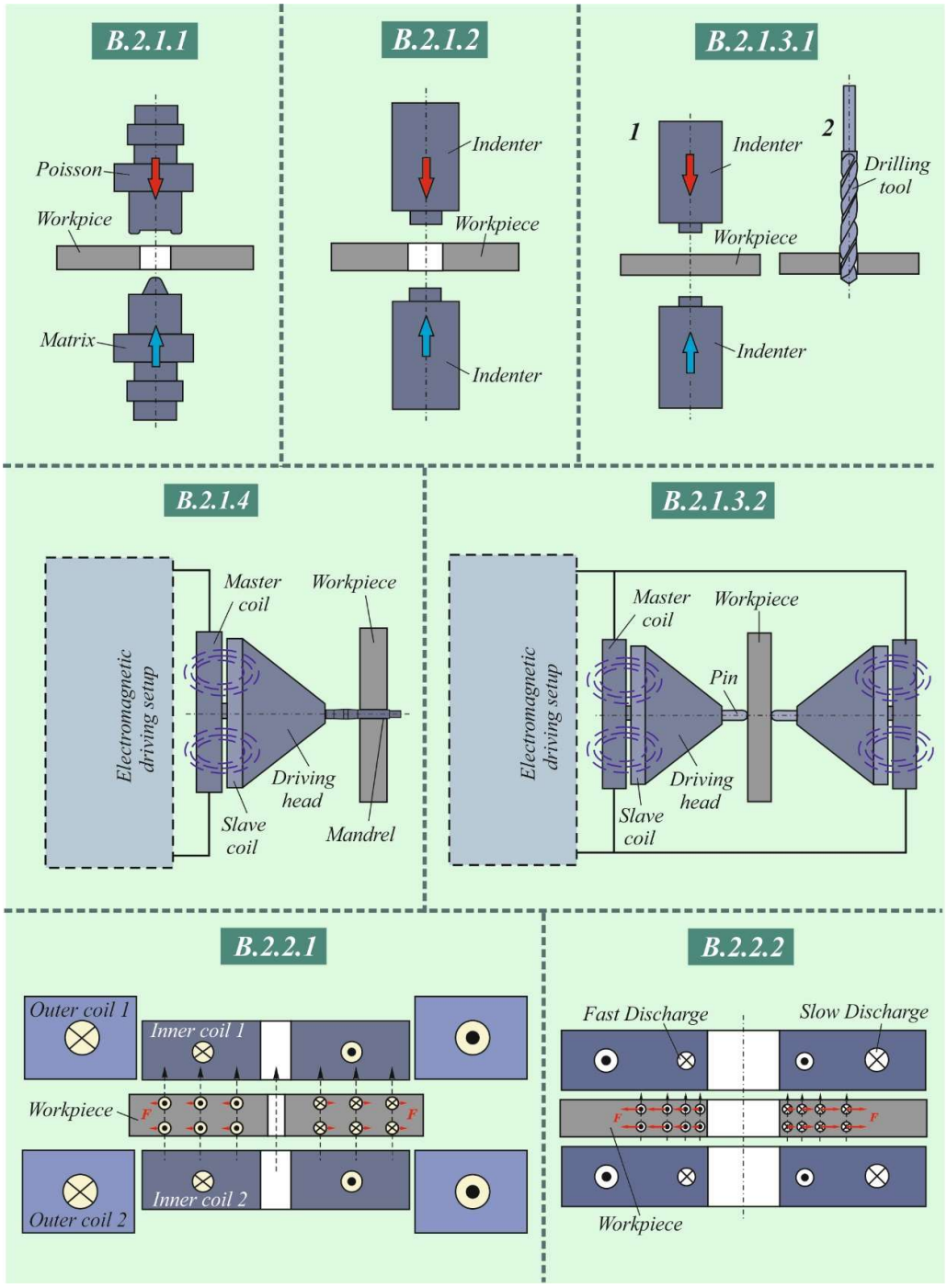

Fig. 1.10 Principal schemes of the dynamic methods for introducing beneficial compressive RSs

1.3.3. Methods for introducing beneficial hoop compressive RSs and improving in SI

The methods of group C (Fig. 1) simultaneously aim at two effects: 1). Introduction of beneficial hoop RSs; 2). Modification of the complex state of the material (SI) around the holes. For this purpose, the methods of this group have a common physical basis: tangential contact exists between

the corresponding tools and the hole surface in both axial and hoop directions. Therefore, the kinematics of the corresponding tools include rotation around the hole axis and translation along this axis. The schematic diagrams of the methods of group C are shown in Fig. 1.11.

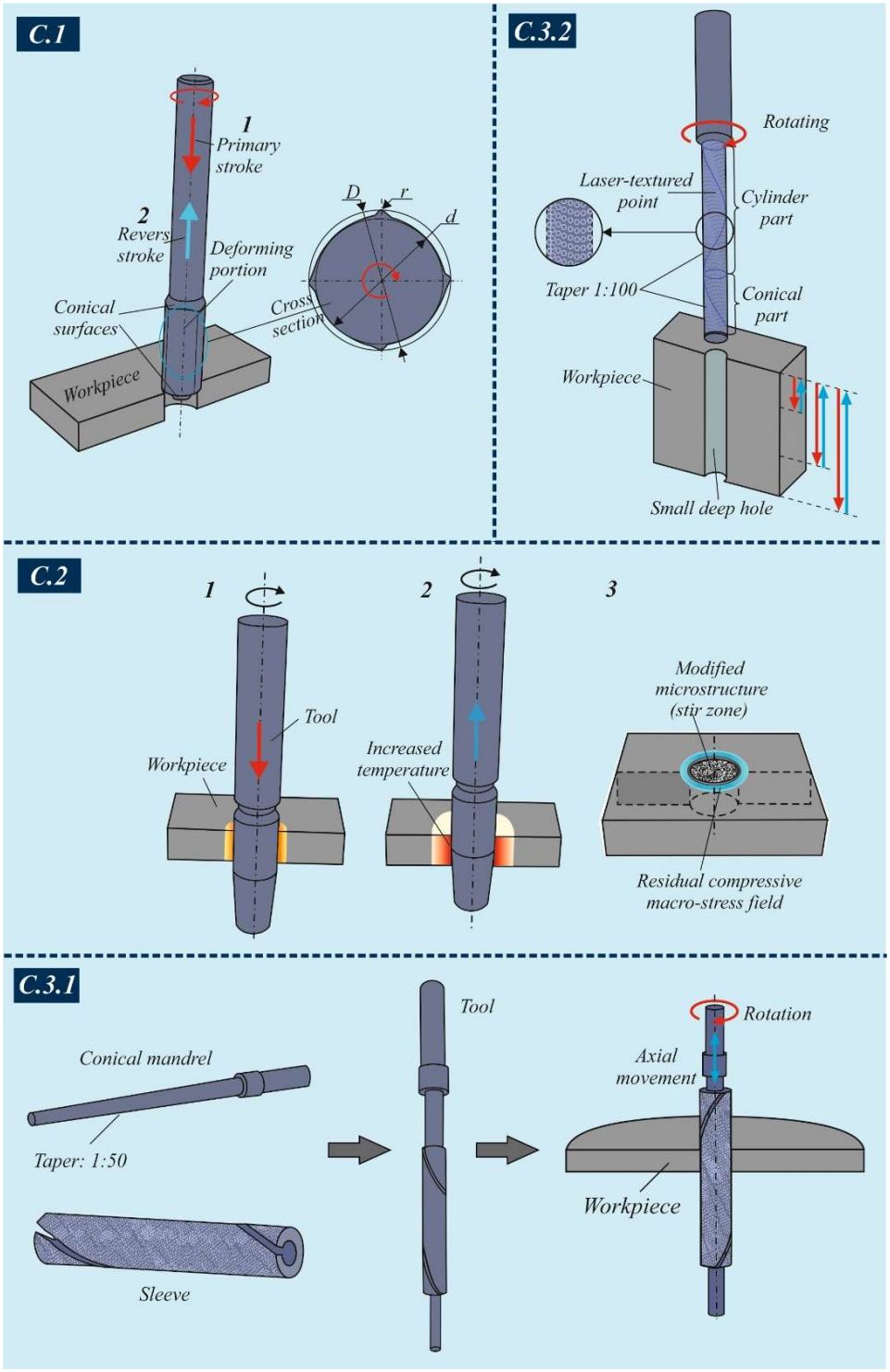

Fig. 1.11 Principal schemes of the methods for introducing beneficial hoop compressive RSs and improving in SI

Chapter 2. NATURE AND REALISATION OF MODIFIED METHOD FOR COLD EXPANSION FASTENER HOLES

2.1. Analysis of the base method SMCW

The basic idea of SMCW to eliminate costly longitudinally cut sleeve with inner oiling for single use in rival method SSCE (fig. 1.9, scheme B.1.1.4), which execute the role of intermediary between cone – cylindrical pin and the surface of the pre-drilled hole in the process of CE. The method is developed to be applied on aluminum alloys used in the aero industry. The analysis conducted of the technological cycle of the basic method SMCW indicates the following:

1) A very narrow tolerance of the diametrical size of pre-drilled holes is necessary which demands implementing countersinking after drilling the holes;

2) The technological cycle consist of a large number of operations (altogether 11 operations) 4 of which a control operations;

3) The stiffness varies in frame tolerance of the diameter of the pre-drilled hole since it defies the difference between diameter d_t of "hardened" mandrel and the diameter of the pre-drilled hole d_o.

4) Highly trained operators are demanded.

For fulfilling conditions 1) – 4) significantly increases the processed cost.

2.2. Nature of the modified Split Mandrel Cold Working (MSMCW) method

The modified Split Mandrel Cold Working (MSMCW) method is developed by Maximov and Duncheva as a counterpart of the displayed above shortcomings of the basic method SMCW. In the base of the MSMCW is the idea of transforming the process of CEH the process from measurable to immeasurable. Tool and devise trough which MSMCW is achieves provide constant stiffness in conditions of relatively wider tolerance of the diameter size of the pre-drilled holes. Under these circumstances, MSMCW method could be applied when the holes are crafted only through drilling. This permits to eliminate countersinking obligatory in the basic method SMCW. In result the total time needed for processing of a hole and the total production costs are being reduced.

2.2.1. Stages of the technological cycle

Fif. 2.3 shows the tool geometry and the main stages for the cold working of holes using the new tool and device. The tool includes a partially longitudinally split mandrel so that at least three symmetrical segments are formed. An axially movable conical–cylindrical pin is positioned in the axial hole of the mandrel. The mandrel working part comprises two conical surfaces connected by a cylindrical surface. The pin's conical surface contacts the surface of a conical hole made in the split end of the mandrel. The two conical surfaces have the same angle of inclination α and are widening on direction the cut end of the mandrel.

The procedure for the proposed method contains the following stages: (fig. 2.3):

Stage I: *Inserting the mandrel into the pre-drilled hole.* (fig. 2.3.a).

Stage II: *Compensation for the clearance between the cylindrical surface of the mandrel and the drilled hole.* (fig. 2.3 b).

Stage III: *Cold working* (fig. 2.3.c).

Stage IV: *After the tool exits the hole, the plastically deformed layer of metal around the hole and creating an area of useful hoop residual stresses around the hole* (fig. 2.3. d).

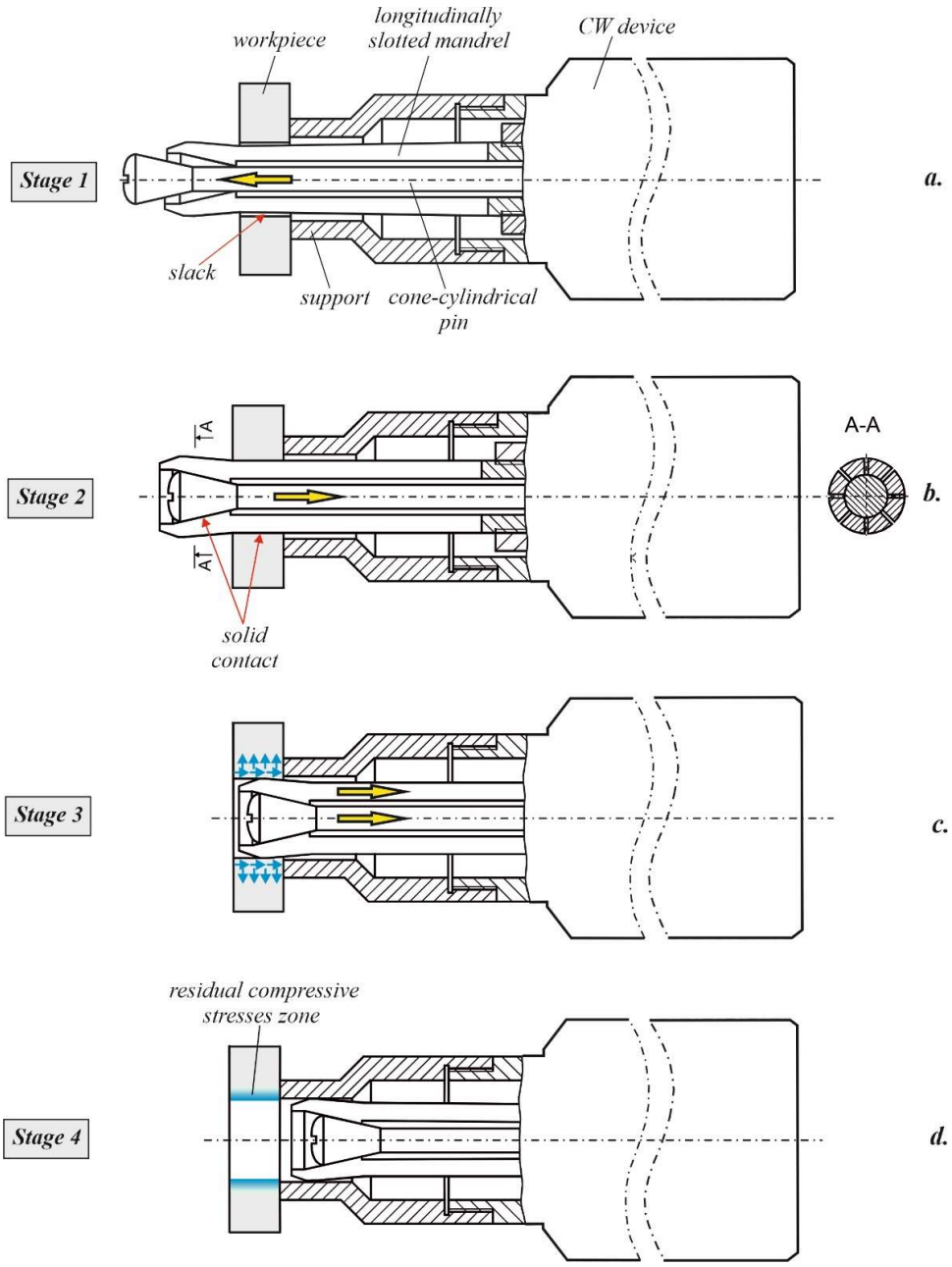

Fig. 2.3. Basic stages of the technological cycle for cold expansion of holes via the modified split mandrel method

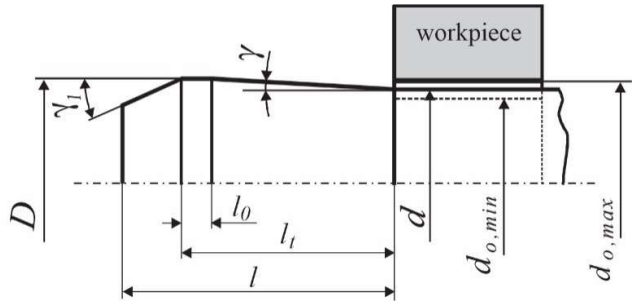

Fig. 2.4. Geometric parameters of the mandrel

The presence of hard contact achieves constant tightness during the cold-working process CPO since the tightness depends only on the difference between the mandrel's major diameter D and the diameter d f its cylindrical surface (fig. 2.4);

2.2.2. Geometric parameters of the mandrel

After ensuring hard contact (i.e., completing Stage II), the tightness during the cold working

is a constant (fig. 2.4):

$$i = D - d = const \tag{2.2}$$

The DCE is equal to the hoop linear strain ε_t for the points on the hole surface. The DCE limits are defined by the minimum and maximum allowable diameters of drilled holes, $d_{o,min}$ and $d_{o,max}$ (fig. 2.4):

$$DCE_{min} = \varepsilon_{t,min} = \frac{i}{d_{o,max}} \times 100,\% \tag{2.3}$$

$$DCE_{max} = \varepsilon_{t,max} = \frac{i}{d_{o,min}} \times 100,\% \tag{2.4}$$

Formulas (2.3) and (Fig. 2.4) show that the dispersion of the DCE is negligible compared to the significantly larger range of the variation of the DCE is insignificant compared to the relative variation interval of d_o. Therefore, the wide tolerance of the diameters of the pre-machined holes using the MSMCW method results in a relatively small change in the DCE.

For an unhindered insertion of the split mandrel into the pre-drilled holes, the following geometric condition must be met:

$$\sqrt{D^2 - \delta^2} - \frac{\delta}{\mathrm{tg}\left(\frac{180}{n_s}\right)} \leq d_{o,min} \tag{2.5}$$

2.3. Tool and device implementing the MSMCW method:

The tool implementing the MSMCW is shown on Fig. 2.5.

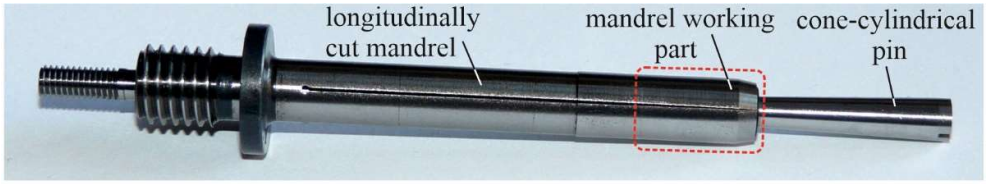

a.

b.

Fig. 2.5. The tool implementing, MSMCW process:

The longitudinally split mandrel and the conical–cylindrical pin were fixed to the device via threads. Four symmetrical segments were formed in the partially longitudinally split mandrel, and the width of the sections in the mandrel was $\delta = 0.5\ mm$ The components of the tool in the front position and the rear (working) position of the pin relative to the split mandrel are shown in fig. 2.5a and 2.5b, respectively..

Clearance exists for all treated holes, with the exception of those machined at the upper limit of the diametral size. The geometric parameters of the working part of the split mandrel in accordance with the notations from Fig. 2.4 are shown in Table 2.1:

Geometric parameters of the working part of the split mandrel *Table 2.1.*

d, mm	D, mm	l_t, mm	l_o, mm	L, mm	γ, deg	γ_1, deg	δ, mm
8.05	8.37	2	11.17	13.4	1	10	0.5

For the interference fit i, the following applies:

$$i = D - d = 8.37 - 8.05 = 0.32\ mm = const \quad (2.6)$$

For the specified geometric parameters in Table 2.1, number of segments of the split mandrel $n_s = 4$ and for $d_{0,min} = 8.00\ mm$ the condition for unimpeded entry of the tool into the holes is met.:

$$\sqrt{8.37^2 - 0.5^2} - \frac{0.5}{tg\frac{\pi}{4}} = 7.855\ mm < d_{0,min} \quad (2.7)$$

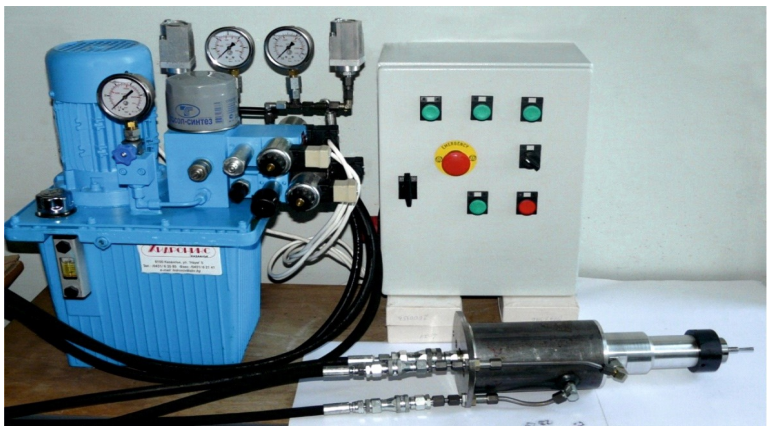

A general view of the device with hydraulic drive and the tool, realizing the technological cycle of MSMCW in accordance with stages I-IV, is shown in Fig. 2.6.

Fig.2.6 General view of the cold-working device with tool, hydraulic station, and control module.

2.4. Conclusions

► The conducted comparative analysis of the technological cycles used in the competitive methods SSCE and SMCW confirms that they implement fundamentally the same concept: a dimensional CEH respectively a very narrow tolerance of the pre-machined holes in conditions of unilateral access to the corresponding components. This reflects on: 1) a large number of operations, including counterboring and control operations; 2) the interference fit is a variable within the tolerance of the pre-machined holes; 3) significantly more time and production costs;

► The modified method combines the competitive advantage of the basic SMCW method for eliminating the expensive longitudinally split single-use intermediate sleeve with the possibility of CEH in conditions of a relatively wide tolerance of the diameter of the pre-drilled holes. This provides the following advantages of MSMCW compared to the basic method: 1) Fewer operations due to the elimination of hole counterboring and two control operations based on the geometric criteria of the holes and the working part of the tool; 2) Ensuring CEH with constant interference fit; 3) Well-trained operators are not required; 4) Significantly less time and overall production costs;

► A functionally linked tool designed for stressing holes with a nominal hole diameter of $d_o = 8\ mm$ and a device with a hydraulic drive, realizing MSMCW, have been designed and manufactured.

Chapter 3. EFFICIENCY OF THE MSMCW METHOD FOR IMPROVING SURFACE INTEGRITY IN BUSH-TYPE SPECIMENS FROM 2024-T3 ALUMINUM ALLOY

3.1. Main purpose

The aim of the study is to evaluate in quantitative and qualitative aspects the efficiency of the MSMCW method in terms of the main characteristics of the SI, which are crucial for improving the fatigue behavior of structural elements with FH. Such characteristics are the distribution of the hoop RSs, the microstructure, and the microhardness profile of the material around the holes. Taking into account the ability of the MSMCW method to compensate for the initial clearance between the hole

surface and the tool, the change in the specified SI characteristics was studied under conditions of a relatively wide tolerance of the diameter of the pre-drilled holes.

3.2. Materials and Methods

3.2.1. Materials

The material under test was aluminum alloy 2024-T3, obtained as (1) hot-rolled bars with a diameter of 32 mm. An optical emission spectrometer was used to determine the chemical composition, with the minimum value of the step for determining the content of chemical elements in weight percentages being 0,001. The chemical composition of the alloy is shown in table 3.1.

Chemical composition of 2024-T3 aluminum alloy in the form of bar *Table 3.1.*

Al	*Si*	*Fe*	*Cu*	*Mn*	*Mg*	*Zn*	*Cr*
94.03	*0.746*	*0.485*	*1.64*	*0.764*	*1.67*	*0.0192*	*0.0382*
Ni	*Ti*	*Be*	*Ca*	*Li*	*Pb*	*Sn*	*Sr*
0.0186	*0.0280*	*<0.0001*	*>0.0200*	*0.0025*	*0.237*	*0.0237*	*0.0004*
V	*Na*	*Bi*	*Zr*	*B*	*Ga*	*Cd*	*Co*
0.0106	*0.0156*	*0.0203*	*0.0074*	*<0.0005*	*0.0237*	*<0.0010*	*<0.0020*
Ag	*Hg*	*In*	*Sb*	*Ce*	*La*	*Mo*	*Sc*
0.0018	*<0.0050*	*0.0116*	*0.140*	*0.0197*	*0.0055*	*0.0037*	*<0.0005*

3.2.2. Experimental samples

The experimental specimens were bushing type with the following nominal overall dimensions: outer diameter $D = 32\ mm\ and\ thickness\ \delta = 6\ mm$. To evaluate the influence of the scattering of the pre-drilled hole diameter, the tests were carried out on four samples whose holes were successively drilled and reamed to obtain the following nominal diameters. The axisymmetric geometry of the specimens ensures correct conclusions regarding the influence of the process parameters on the distribution of the RSs, the microhardness profile, and the microstructure.

3.2.3. Methods of investigation

3.2.3.1. X-ray diffraction analysis for measuring residual stresses

The objects of measurement are the hoop RSs on the front faces of the specimens in the radial direction from the edge of the hole along the entry and exit sides of the tool. A D8 ADVANCE diffractometer with a pin-hole collimator with a $\emptyset 1.0\ mm$ was used to measure the residual stresses. The mode of operation of the X-ray tube (high voltage/current) was 30 kV/ 40 mA. The $sin^2\psi$ method and a numerical procedure based on the method of least squares were used.

The measured diffraction profile of the Al {311} plane had a maximum at $2\theta \approx 139.3°$ for the used chromium radiation filtered by a VKα filter. The diffraction profiles were determined via the Pearson VII method, calculating the deformations of the aluminum alloy lattice in the Al {311} direction. The Winholtz–Cohen method was applied for the generalized Hooke's law with the following elastic constants: $s_1 = -4.514\ TPa^{-1}$ and $\frac{1}{2}s_2 = 18.19\ TPa^{-1}$. The following parameters were used in the experiment: 2θ range of $135° - 143°$, 2θ step of 0.5° and a slope defined via$sin^2\psi$ = 0, 0.1, 0.2, 0.3, 0.4, 0.5 f or both positive and negative values of the angle ψ. The effective penetration depth of CrKα radiation was in the range $6.5 - 11.0\ \mu m$. The experimental setup for X-ray diffraction analysis is shown in fig. 3.1 a, b.

Fig. 3.1 Experimental setup for X-ray diffraction analysis

- **3.2.3.2. Microstructure analysis**

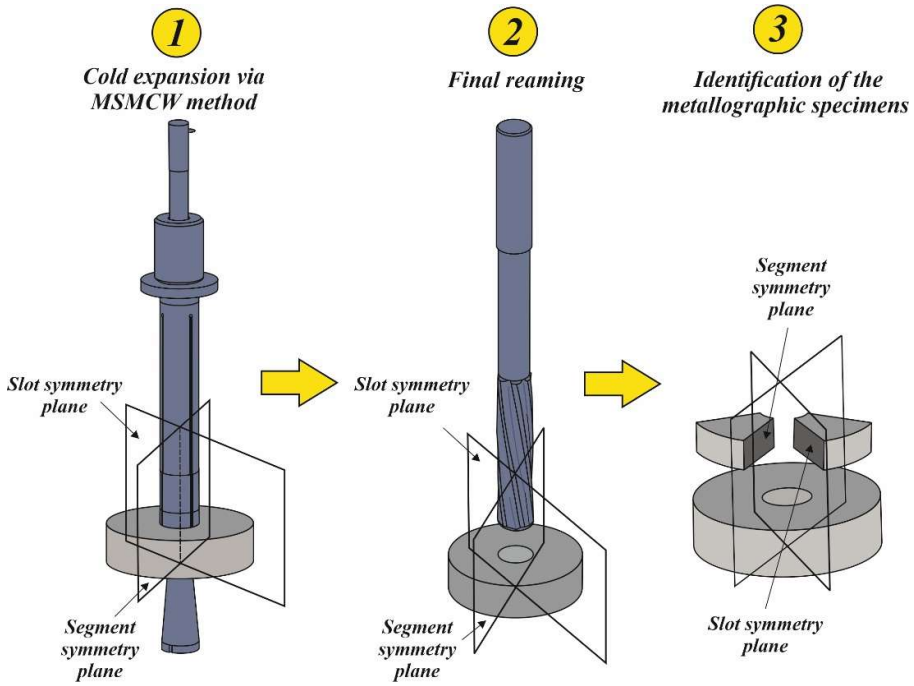

Fig. 3.2 Scheme for the identification of polished mounts used for microstructure and microhardness analysis

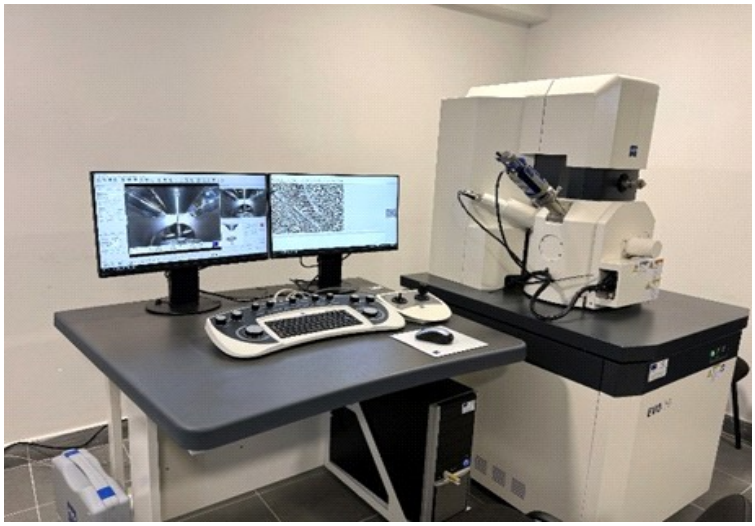

Fig. 3.3 Scanning Electron Microscope Zeiss Evo 10

A EURO-MEX IM-Series metallographic microscope, equipped with a CMEX Pro 5 camera, and a Zeiss Evo 10 Scanning Electron Microscope (SEM) were used for the metallographic analysis.

For the investigation of the microstructure, polished mounts were prepared in the front planes and in axial sections of the samples.

The metallographic optical microscope was used for microstructure analysis in the front planes of the samples.

SEM was used for the microstructure analysis in axial sections, corresponding to the plane of symmetry of the segments and the plane of symmetry of the cuts of the split mandrel. The polished mounts in axial sections were prepared in segments cut from the samples according to the scheme shown in fig. 3.2. These polished mounts were also used for measuring the microhardness in axial sections (see item 5.2). The operating mode of the SEM was in a high vacuum environment, with a current magnitude of I=200 pA and a voltage of U=20 kV. A photo of the SEM used is shown in fig. 3.3.

3.2.3.3. Microhardness measurement

For measuring the microhardness, two types of polished mounts were prepared: 1) In the front planes of the samples; 2) In axial sections of segments cut from the samples in accordance with the scheme shown in fig. 3.2 For a comparative investigation of the microhardness, three samples were manufactured: a sample without a hole for evaluating the microhardness in the as-received condition, and two samples with different diameters of pre-processed holes – specifically $d_o = 8.14\ mm$ and $d_o = 8.30\ mm$, obtained after reaming.

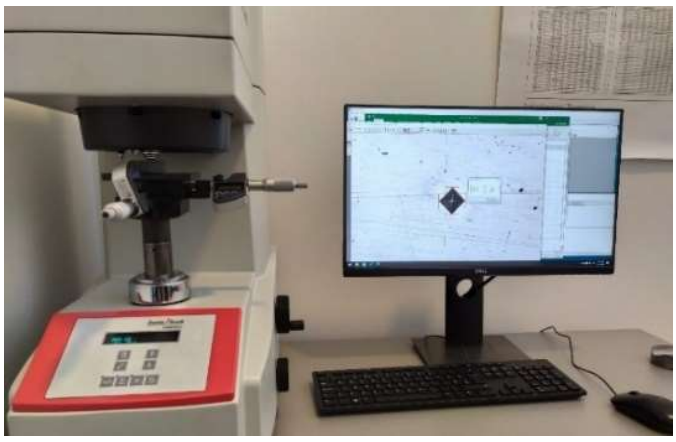

Fig. 3.4 Microhardness tester Zwick/Indentec-ZHVμ-S

The object of comparison in the two front planes of the samples is the microhardness profiles in the radial direction. These profiles were obtained as an arithmetic average value across four directions, located in two perpendicular planes, starting from points close to the edge of the holes. For the two samples with CEH these planes correspond to the planes of symmetry of the segments and the planes of symmetry of the cut.

The purpose of the microhardness measurement in the axial sections is to compare the microhardness at different initial hole diameters ($d_o = 8.14\ mm$ and $d_o = 8.30\ mm$) in the two characteristic planes of the samples, corresponding to the plane of symmetry of the segments of the

split mandrel and the plane of symmetry of the cuts of the same (fig. 3.2). The object of measurement is the microhardness in the radial direction near the two front faces of the samples.

A semi-automatic microhardness tester *Zwick/Indentec-ZHVμ-S* (fig. 3.4) was used for measuring the microhardness. To measure the microhardness as close as possible to the edge of the hole, a load of 10 g was used.

3.3. Efficiency of the MSMCW method on the distribution of RSs

3.3.1. Experimental setup

To evaluate the influence of the scattering of the pre-drilled hole diameter, the tests were carried out on four samples whose holes were successively drilled and reamed to obtain the following nominal diameters: $d_o = 8.14, 8.16, 8.20, 8.30\ mm$ (fig. 3.5a, b, c, d). The front planes of the samples were polished.

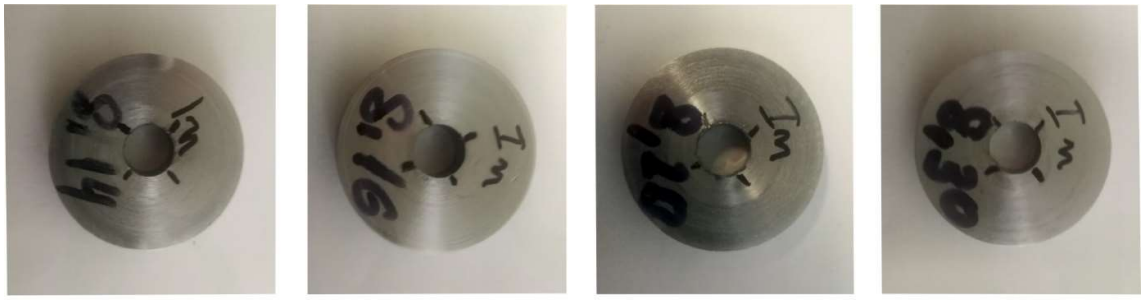

a. *b.* *c.* *d.*

Fig. 3.5. Experimental specimens for studying the residual hoop stress evolution

According to formulas (2.3) and (2.4), the DCE limits were as follows:

$$DCE_{max} = \varepsilon_{t,max} = \frac{i}{d_{o,min}} = \frac{0.32}{8.14} \times 100 = 3.93\ \%$$

$$DCE_{min} = \varepsilon_{t,min} = \frac{i}{d_{o,max}} = \frac{0.32}{8.30} \times 100 = 3.85\ \%.$$

After cold working CEH, the holes were further machined by sequential reaming to obtain the following diameters: $d = 8.4,\ 8.5,\ 8.6\ mm$. Thus, the influence of the thickness of the metal's cut layer around the stressed holes on the redistribution (evolution) of residual hoop stresses could be evaluated in correlation with the diameters d_o.

3.3.2. Influence of the scattering (DCE) of pre-processed holes on residual hoop stress distribution after cold working CEH

Fig. 3.6a, b, c, d visualizes the influence of the scattering of the pre-drilled hole d_o, respectively the effect of varying the DCE, on the distribution of the residual hoop stresses, obtained immediately after the CEH. The experimental results give rise to the following comments:

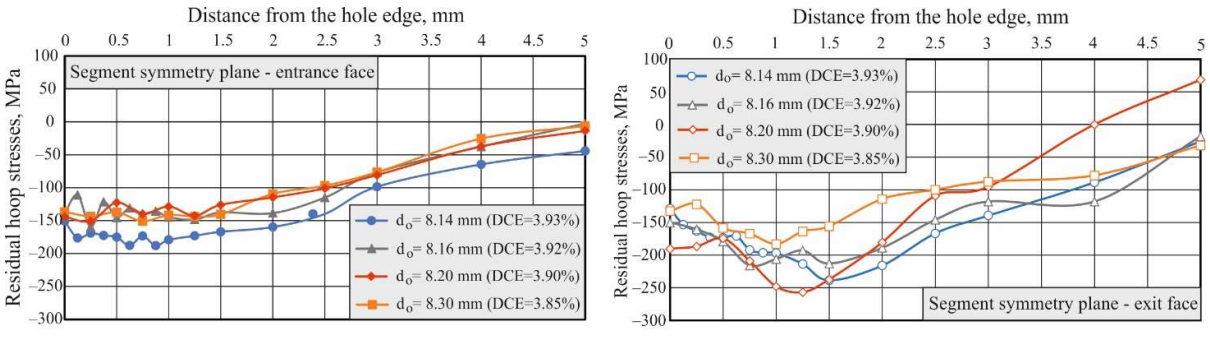

a. b.

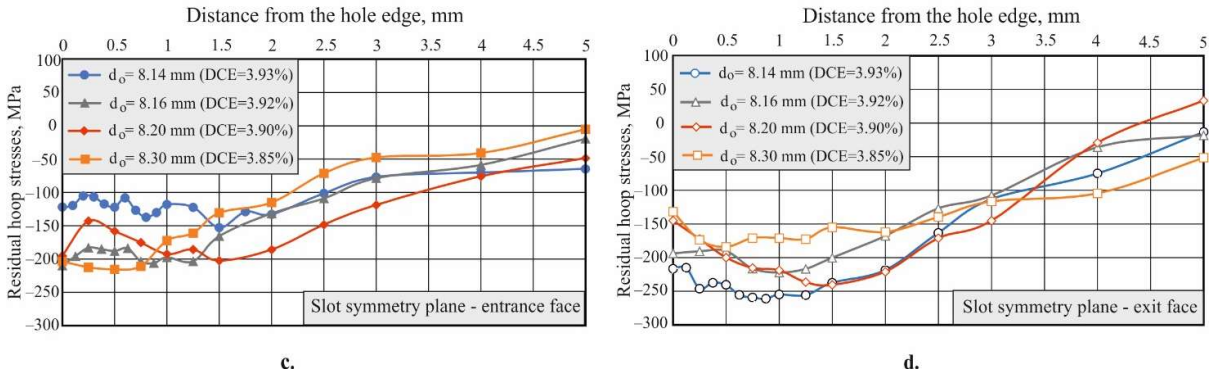

Fig. 3.6 Influence of the scattering (DCE) of pre-processed holes on residual hoop stress distribution after cold working CEH

3.3.3. Evolution of the residual hoop stress depending on the thickness of the cut metal layer around the hole

Fig. 3.7a, b, c, d shows the residual hoop stress distribution for a sample with an initial hole diameter $d_o = 8.16\,mm$ after drilling and reaming, and its evolution after cold working CEH and successive reaming to achieve holes with diameters $d = 8.4, 8.5, 8.6\ mm$.

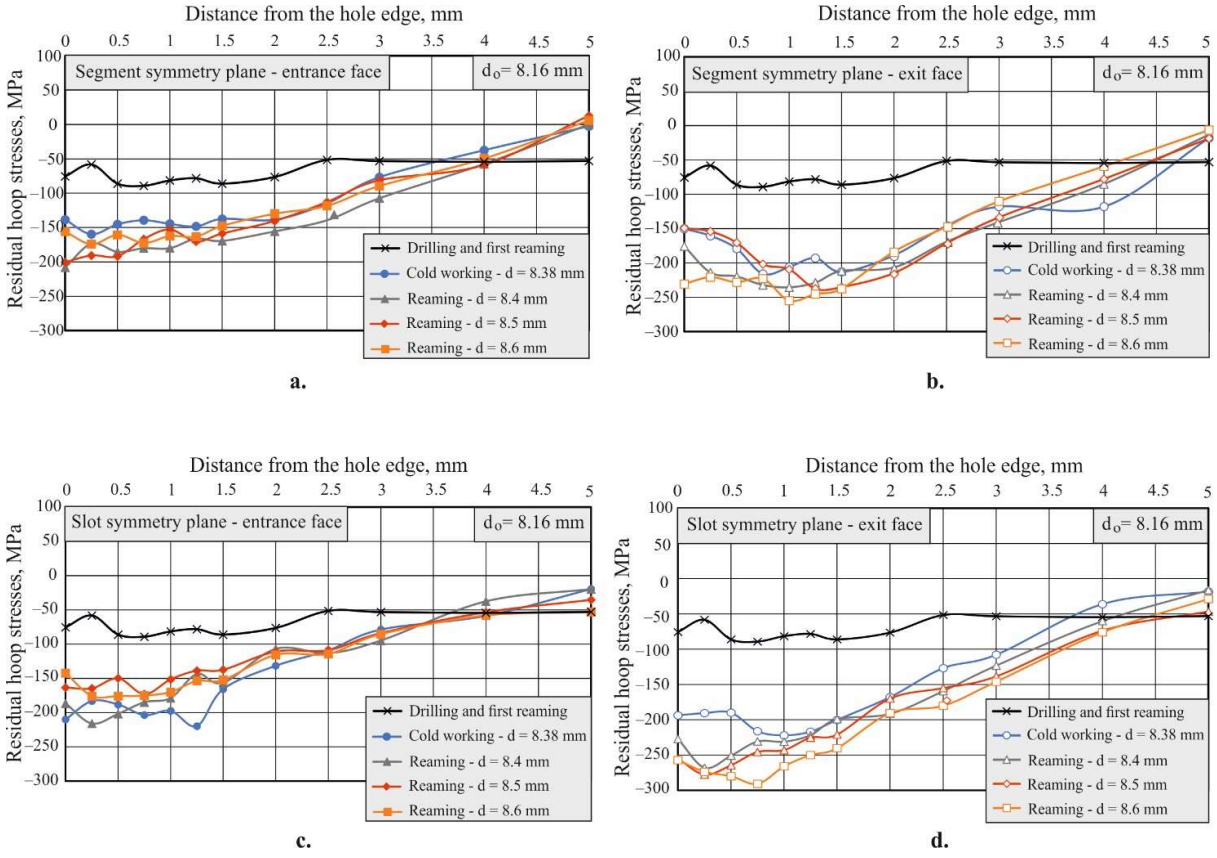

Фиг. 3.7 Evolution of the residual hoop stress distribution after cold working CEH and consecutive reaming of the holes

3.3.4. Influence of premachined hole diameter dispersion (DCE) on the final residual hoop stress distribution

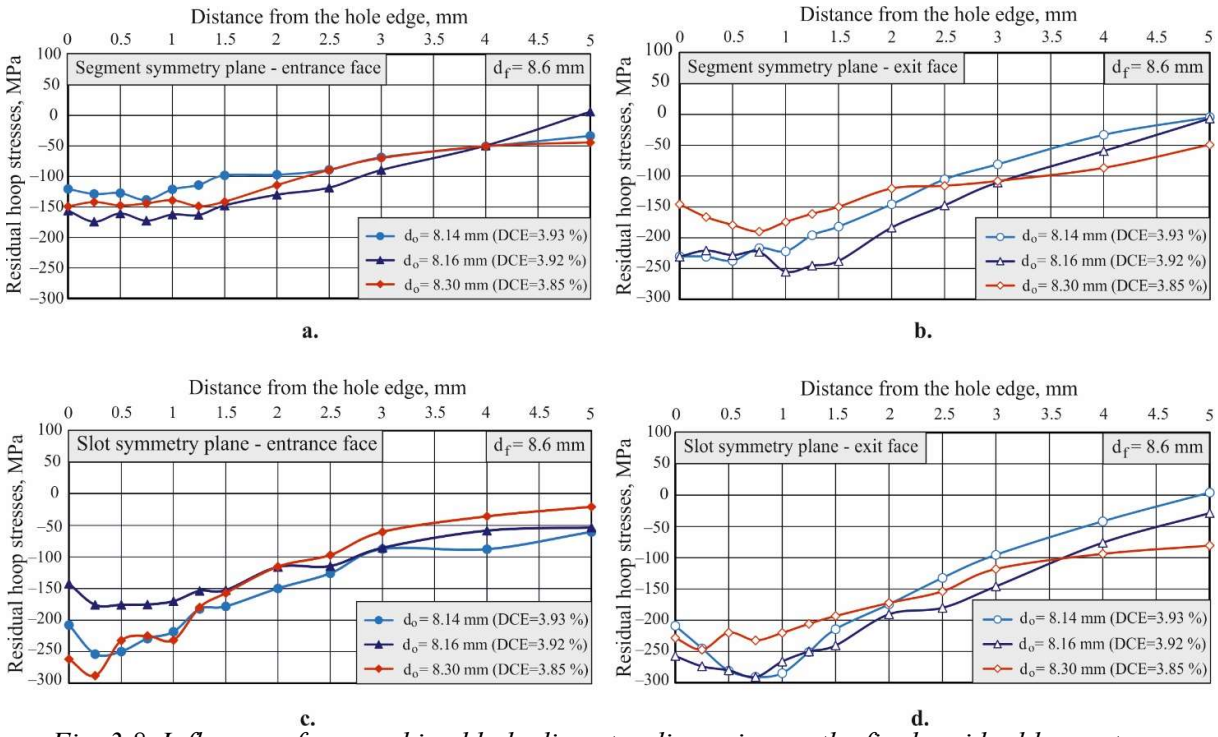

Fig. 3.8. Influence of premachined hole diameter dispersion on the final residual hoop stress distribution

Fig. 3.8a, b, c, d visualizes the final residual hoop stress distribution in the two characteristic planes of symmetry on the input and output sides of the samples depending on the diameter of the pre-processed hole d_o.

3.4. Influence of the MSMCW method on the microstructure

3.4.1. Microstructure in cross-sections

Fig. 3.9 Samples for microstructure analysis in cross-sections.

For the microstructure analysis in the front planes of the samples, 4 polished mounts were prepared, corresponding to the following four stages: 1) In the as-received condition (without a hole); 2). After drilling and reaming the hole; 3) After CEH, using the tool and device realizing the MSMCW process; 4) After final reaming of the hole. The polished mounts were made on the front face, corresponding to the entry side of the CEH and the reamers. The prepared test specimens are shown in fig. 3.9.

Optical images of the microstructure for the indicated stages and characteristic planes after CEH at magnifications of $\times$ 200 and $\times$ 500 respectively, are shown in fig. 3.11 – fig. 3.14.

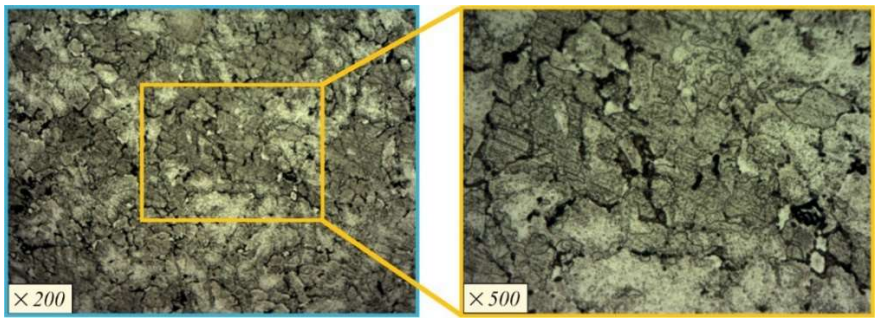

a. *b.*

Fig. 3.10 Optical images of the microstructure in the as-received condition

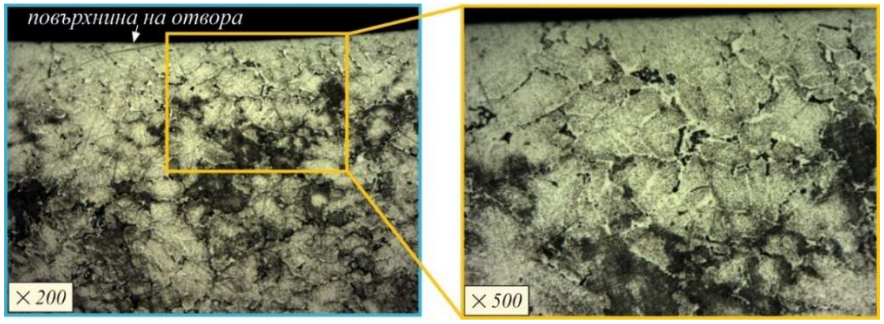

a. *b.*

Fig. 3.11 Optical images of the microstructure after drilling and reaming the hole

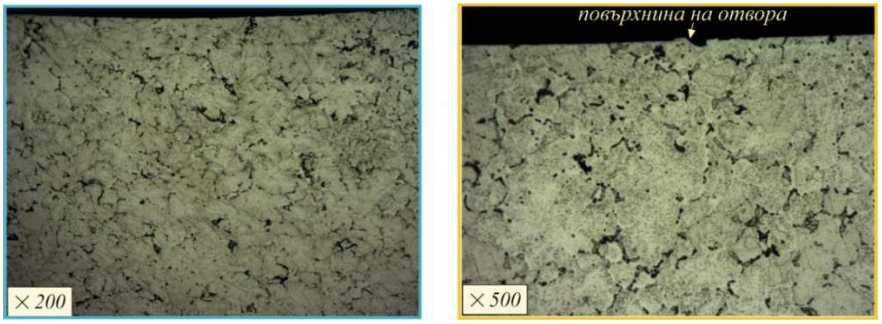

a. *b.*

Fig. 3.12 Optical images of the microstructure after CEH in the zone of the plane of symmetry of the segment

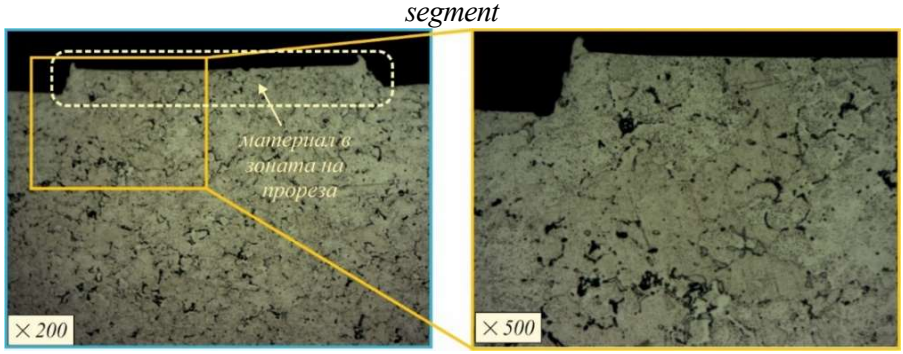

a. *b.*

Fig. 3.13 Optical images of the microstructure after CEH CPO in the zone of the plane of symmetry of the notch

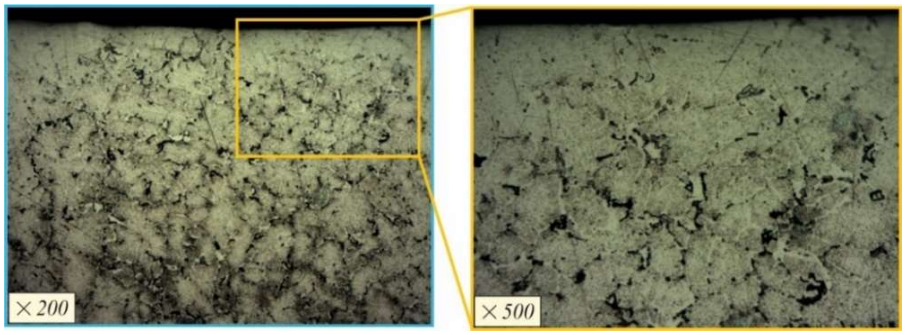

a. *b.*

Fig. 3.14 Optical images of the microstructure after final reaming of the hole

A highly deformed layer is observed in the zone of the plane of symmetry of the segment (fig. 3.12a, b), while a thin strip of material undeformed in the radial direction is expectedly observed in the zone of the plane of symmetry of the notch, as it does not come into direct contact with the tool (fig. 3.13).

- **3.4.2. Microstructure in axial cross-sections**

The experimental specimens are bushing type with the following nominal overall dimensions: outer diameter $\emptyset\, 32\ mm$ and thickness $6\ mm$ with pre-drilled holes with diameters obtained after reaming, respectively $d_o = 8.14\ mm$ and $d_o = 8.30\ mm$. After cold working through MSMCWmethod, the holes were further machined by sequential reaming to obtain the following diameters $8.5\ mm$ (fig. 3.15).

a. *b.*

Fig. 3.15 Experimental specimens for studying the microstructure and microhardness in axial sections

Fig. 3.16a, b shows the microstructure at different magnifications of the sample with an initial hole diameter of $d_o = 8.14\ mm$, in an axial section corresponding to the plane of symmetry of the tool's notch. Fig. 3.17 shows SEM images of the microstructure of the sample with an initial hole diameter of $d_o = 8.14\ mm$, in the zone deformed by the middle of the segment of the cut mandrel.

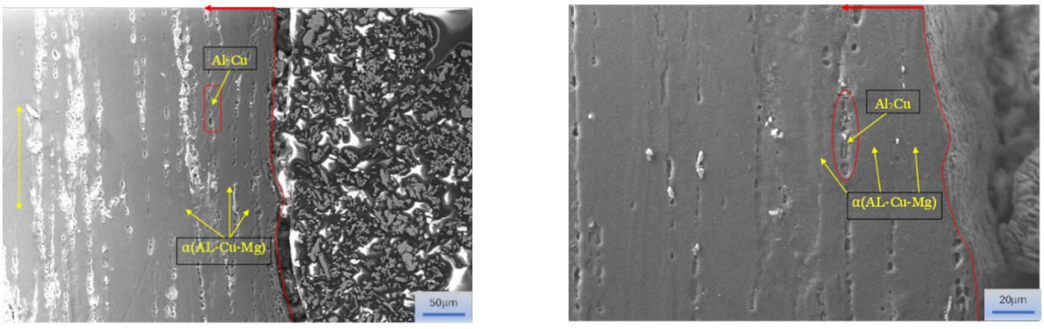

a. *b.*

Fig. 3.16 SEM images of the microstructure of the sample with an initial hole diameter of 8.14 mm, in the zone corresponding to the middle of the tool's notch

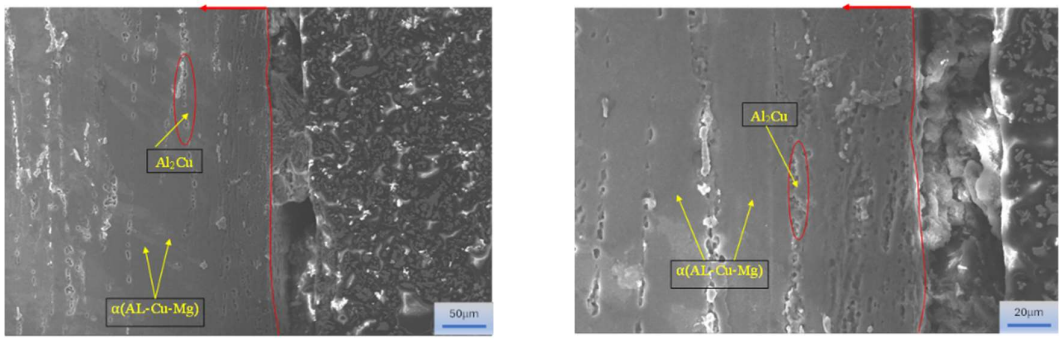

a. *b.*

Fig. 3.17 SEM images of the microstructure of the sample with an initial hole diameter of 8.14 mm, in the zone deformed by the middle of the tool's segment

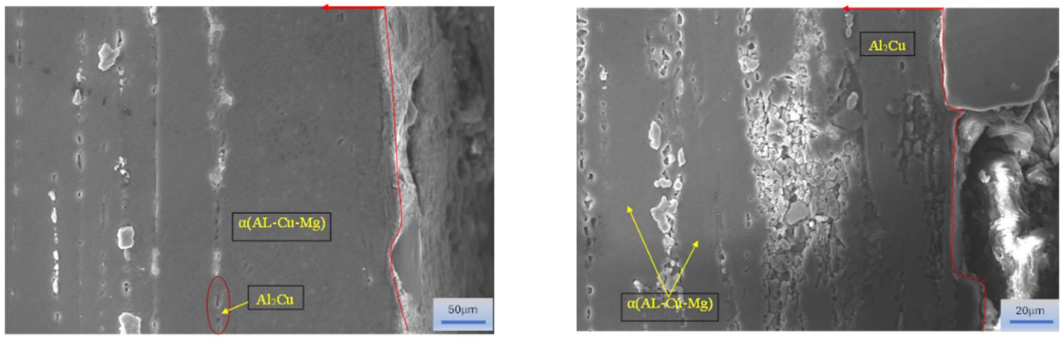

a. *b.*

Fig. 3.18 SEM images of the microstructure of the sample with an initial hole diameter of 8.30 mm, in the zone corresponding to the middle of the tool's notch

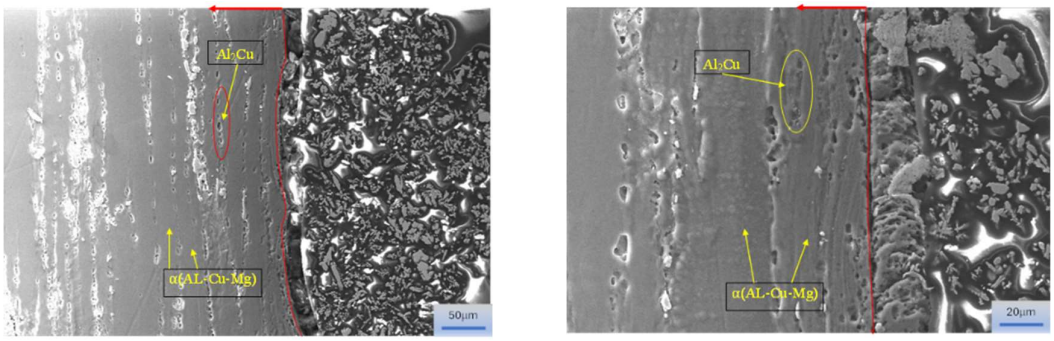

a. *b.*

Fig. 3.19 SEM images of the microstructure of the sample with an initial hole diameter of 8.30 mm, in the zone deformed by the middle of the tool's segment

Fig. 3.18a, b (5) shows the microstructure at different magnifications of the sample with an initial hole diameter of $d_o = 8.30\ mm$, in an axial section corresponding to the middle of the tool's notch, while fig. 3.19a, b shows SEM images of the microstructure of the same sample in the zone deformed by the middle of the segment of the cut mandrel.

In the observed structures, a fibrous $\alpha - Al$ phase (solid solution of $Al,\ Cu,\ Mg$) and an intermetallic compound Al_2Cu (θ phase) are observed. Precipitations of the θ phase are noted along the grain boundaries. In the zone near the hole, grain refinement (fig. 3.16) is observed.

Fig. 3.18a, b (5) shows the microstructure at different magnifications of the sample with an initial hole diameter of $d_o = 8.30\ mm$, in an axial section corresponding to the middle of the tool's notch, while fig. 3.19a, b shows SEM images of the microstructure of the same sample in the zone deformed by the middle of the segment of the cut mandrel. In the microstructures of the sample with an initial hole diameter of $d_o = 8.30\ mm$ phases analogous to those in the sample with a smaller initial

diameter ($8.14\ mm$) are observed. In this sample, thinning of the α-Al fibrous phase and partial change in the orientation of the grains relative to the hole axis are observed, due to the plastic deformation caused by the middle of the tool's segment (fig. 3.19). the zones far from the hole surface, no phase and structural changes are observed for either sample.

3.5. Influence of the MSMCW method on microhardness

3.3.1. Microhardness in face planes

Fig. 3.20 shows the profiles of the arithmetic mean microhardness of the sample in the as-received condition and of the two samples with initial hole diameters of $d_o = 8.14\ mm$ and $d_o = 8.30\ mm$ respectively. The observed tendency of the microhardness of the base sample increase from the center towards the outer cylindrical surface is a result of the strengthening of the outer layers during the rolling of the bar billets. The graphs show that the effect of the CEH is clearly expressed at a distance of more than *5 mm* from the edge of the holes, both for the input surface (fig. 3.20a), and the output surface (fig. 3.20b) of the samples.

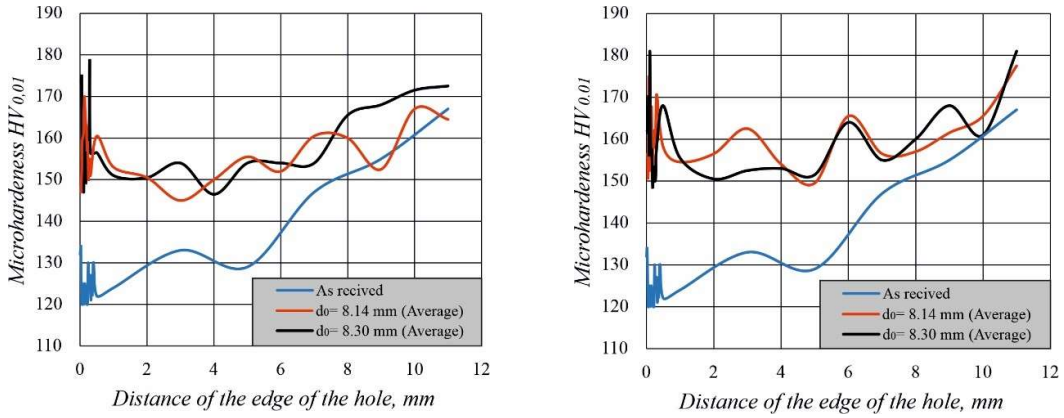

Fig. 3.20 Arithmetic mean microhardness in the radial direction from the edge of the hole; a.) input surface; b.) output surface

3.5.2. Microhardness in axial sections

Fig. 3.21a,b and 3.22a, b show the microhardness profiles in axial sections in the plane of symmetry of the notch and in the plane of symmetry of the segment near the input and output surfaces of the two samples with an initial hole diameter of $d_o = 8.14\ mm$ and $d_o = 8.30\ mm$ respectively. Immediately next to the input surface of the samples (fig. 3.21a and fig. 3.22a) a larger difference is observed between the microhardness profiles in the two characteristic planes.

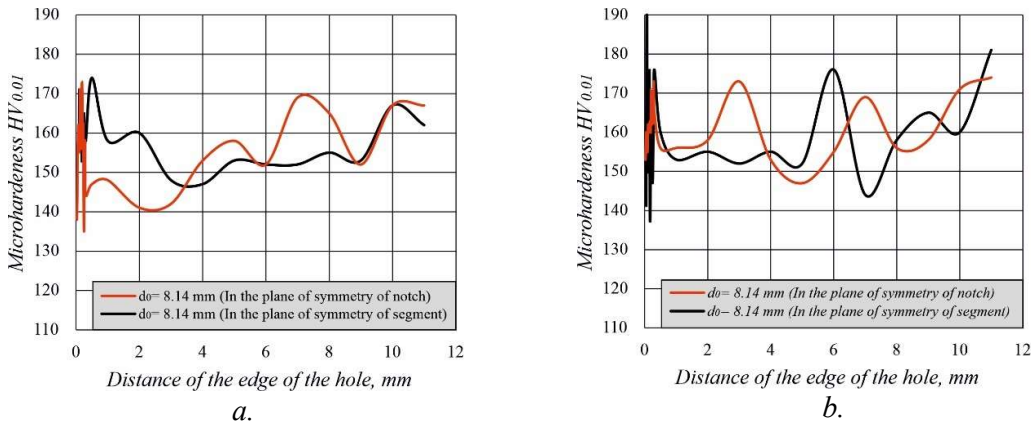

Fig. 3.21 Microhardness in the radial direction from the edge of the hole, at initial diameter $d_o = 8.14\ mm$; a.) input surface; b.) output surface

At a distance of approximately $0.20\ mm$ from the edge of the hole, in the zone affected by the middle of the segment, the microhardness is greater than that measured in the zone around the edge of the segment. Considering the geometry of the tool implementing the MSMCW, this result is expected, as the equivalent plastic deformation in the plane of symmetry of the segment is greater compared to that in the plane of symmetry of the notch. The gradient in the circumferential direction is more pronounced in the sample with a larger initial hole diameter (fig. 3.22a), and the effect manifests at a greater depth. This is probably due to the smaller amount of material removed during the final reaming. The experimental results for microhardness in fig. 3.21b and fig. 3.22b show that the gradient in the circumferential direction decreases near the output side of the samples.

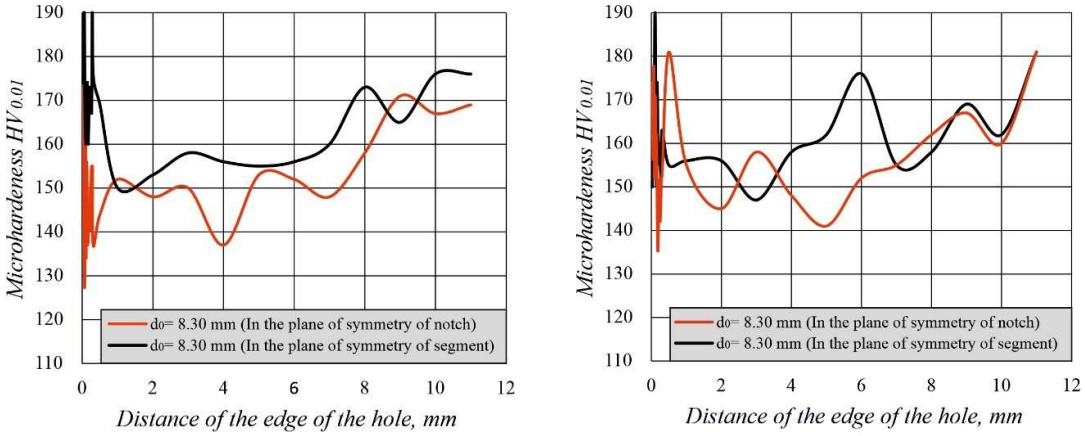

Fig. 3.22 Microhardness in the radial direction from the edge of the hole, at initial diameter $d_0 = 8.30\ mm$; a.) input surface; b.) output surface

3.6. Conclusions

The results of the experimental study conducted of the SI characteristics around the CEH using the MSMCW method provide grounds for the following *main conclusions*:

► The relatively large tolerance on the diameters of the pre-processed holes (0,16 mm at a nominal diameter of 8 mm) leads to dispersion in the distribution of the residual hoop stress, characterized by a gradient in the axial and circumferential directions. Regardless of this, the MSMCW method provides an intensive and deep zone (more than 5 mm) with introduced beneficial compressive hoop residual stresses on both end faces of the samples after CEH and after final reaming of the holes;

► The removal of a plastically deformed layer of appropriate thickness around the hole during final reaming leads to a redistribution of the residual hoop stress around the CEH in the direction of intensifying the compression zone on the input side of the samples. This effect of homogenizing residual stress is a prerequisite for improving the fatigue behavior of 2024-T3 aluminum alloy;

► Microstructure studies near the surface of the holes using the MSMCW method confirm the effect of grain refinement under conditions of different diameters of the pre-processed holes;

► The microhardness on the end faces of a sample in the as-received condition is 25 % lower compared to the microhardness of samples subjected to CEH under conditions of different initial hole diameters. This proves the beneficial effect of work hardening of the material when applying the MSMCW process;

► The microhardness profiles in axial sections confirm the presence of a definite gradient in the circumferential direction, due to the difference in equivalent plastic deformation in the plane of symmetry of the segment and the plane of symmetry of the notch. This effect is more pronounced immediately next to the input side of the samples;

► The experimental results for the SI characteristics correspond to an intentionally used excessively large tolerance on the diameters of the pre-processed holes. Consequently, the application of MSMCW under the usual tolerances for hole diameters in engineering practice will significantly

reduce the dispersion of the SI characteristics around the holes and thereby significantly improve fatigue behavior.

Chapter 4. EFFECTIVNES OF THE MODIFIED SMCW METHOD FOR IMPROVING THE FETIGUE BEHAVIOUR OF 2024-T3 ALUMINUM ALLOY SPECMENTS WITH FASTENER HOLES

4.1. Main purpose

The aim of the present study is to experimentally evaluate the effectiveness of the MSMCW method for increasing the FL of sheet structural elements with FH made of 2024-T3 aluminum alloy, with a view to their application in aircraft construction. In accordance with the main idea of the MSMCW method for compensating the initial clearance between the surface of the pre-drilled holes and the tool, the experimental study was conducted under conditions of a relatively large dispersion of the diameters of the pre-drilled holes, with an emphasis on the repeatability of the results.

4.2. Materials and Methods

4.2.1. Materials

The material is 2024-T3 aluminum alloy in the form of a sheet with a thickness of 5 mm with a chemical composition according to Table 4.1.

Chemical composition of 2024-T3 aluminum alloy in the form of sheet. *Table 4.1.*

Al	*Si*	*Fe*	*Cu*	*Mn*	*Mg*	*Zn*	*Cr*
94.53	*0.784*	*0.445*	*1.62*	*0.79*	*1.48*	*0.0176*	*0.0169*
Ni	*Ti*	*Be*	*Ca*	*Li*	*Pb*	*Sn*	*Sr*
0.0115	*0.0485*	*<0.0001*	*<0.0001*	*0.0026*	*0.126*	*0.0077*	*0.0004*
V	*Na*	*Bi*	*Zr*	*B*	*Ga*	*Cd*	*Co*
0.0108	*0.0024*	*<0.005*	*0.0115*	*<0.0005*	*0.022*	*<0.0010*	*<0.0020*
Ag	*Hg*	*In*	*Sb*	*Ce*	*La*	*Mo*	*Sc*
0.0011	*0.0052*	*0.0113*	*0.132*	*0.0172*	*0.0052*	*0.0026*	*<0.0005*

The mechanical characteristics of the investigated aluminum alloy are summarized based on a uniaxial tensile test of flat specimens. The geometry of the specimens is shown in fig. 4.1.a, and their general view is shown in fig. 4.1.b.

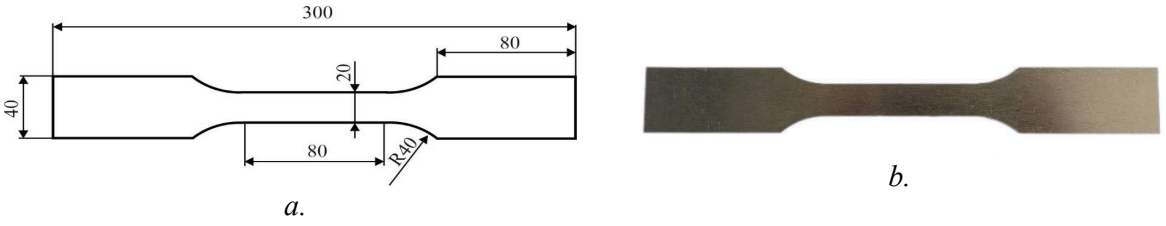

a. *b.*

Fig. 4.1 Geometry of the specimens for tensile tests

To evaluate the effect of the presence of a central hole, the mechanical tensile tests were carried out for two cases—without and with a central hole with a nominal diameter of Ø8.5*mm*. "The presence of a central hole with the specified diameter has little influence on the mechanical behavior of the investigated aluminum alloy under static loading (Table. 4.2.).

Mechanical characteristics of 2024-T3 aluminum alloy without and with hole *Table 4.2.*

Type of Specimens	***$R_{0.2}$, MPa***	***R_m, MPa***	***A_5, %***
Without hole	*319*	*430*	*17,5*
With hole	*331*	*429*	*10,5*

4.2.2. Fatigue specimens

The experimental fatigue specimens have geometric parameters according to fig. 4.1.a with a central hole.

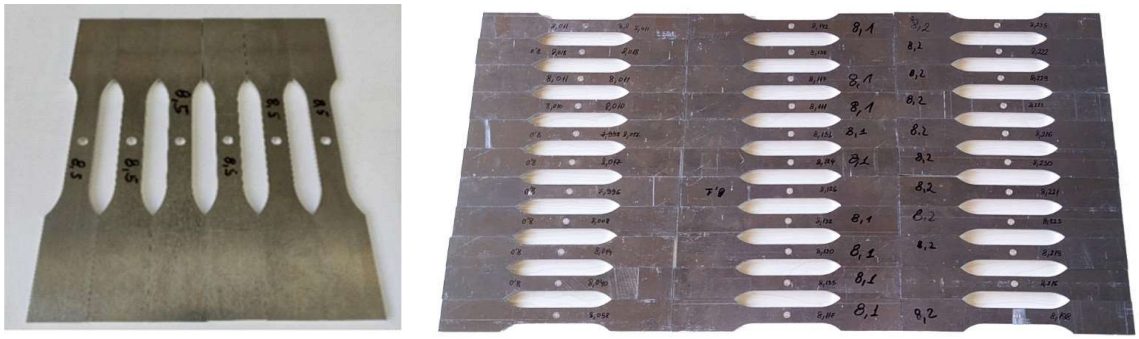

а. *б.*

Fig. 4. Fatigue test specimens: (a) First (reference) group specimens; (b) Second, Third, and Fourth group specimens

The subjects of fatigue tests are four groups of samples, differing in the way the holes are processed:

● Group I (reference) – The holes had a diameter $d_o = 8.5\ mm$ machined by cutting on a milling machining center using interpolation fig. 4.2a;

● Group II. The holes were machined in the following sequence: cutting on a milling machining center to a diameter $d_o = 8.0\ mm$, CEH final reaming to a diameter of $d = 8.5\ mm$ (fig. 4.2б). The holes are cold working with DCE $DCE = \frac{i}{d_0} \times 100 = 0.04 \times 100 = 4\%$;

● Group III. The holes were machined in the following sequence: cutting on a milling machining center to a diameter $d_o = 8.1\ mm$, CEH and final reaming to diameter of $d = 8.5\ mm$ (фиг. 4.2б). The holes were cold working with CEH and $DCE = \frac{i}{d_0} \times 100 = 0.0395 \times 100 = 3.95\%$.

● Group IV. The holes were processed in the following sequence: cutting on a milling machining center to a diameter $d_o = 8.2\ mm$, CEH and final reaming to diameter of $d = 8.5\ mm$ (fig. 4.2б). The holes were cold working with CEH and $DCE = \frac{i}{d_0} \times 100 = 0.039 \times 100 = 3.9\%$.

The MSMCW process was carried out with the same orientation in the hoop direction of the split mandrel: the tool was positioned so that the plane of the critical section of the specimen coincided with the plane of symmetry of any segment. This sequence of hole processing ensures the same final hole diameter and, thus, the same critical section of the fatigue specimens of all groups. On this basis, the following comparative assessments could be conducted:

1). Evaluating effect of the MSMCW method for CEH based on comparison of Groups II, III, and IV with Group I, i.e., with the conventional case of machining the holes by cutting only (drilling and reaming);

2). Evaluating the effect of scattering of the pre-drilled hole diameters before cold working CEH on the fatigue behavior of the respective samples of Groups II, III, and IV;

3). Evaluating the repeatability of the fatigue behavior to a workpiece, treated in the same way

4.2.3. Fatigue tests

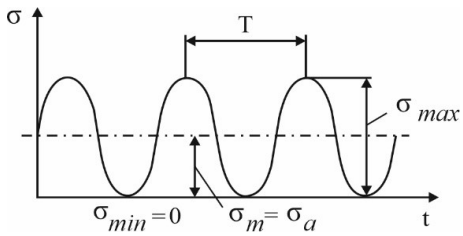

Fig. 4.3 Pulsating cycle, R=0

The fatigue behavior of the specimens from each group was investigated via pulsating cycle fatigue tests since it is the most severe of all tensile fatigue test ($R = 0$, fig. 4.3).

Fig. 4.4 Zwick/Roell Vibrophore 100 testing machine in dynamic mode of operation.

A Zwick/Roell Vibrophore 100 testing machine in the dynamic mode operation was used (fig. 4.4) fatigue tests were performed at a frequency corresponding to a selected resonance frequency by the testing machine. Since all the samples had the same nominal dimensions (including the hole diameters achieved by the final reaming) and were fixed in the same way in the testing machine working bodies, their natural frequencies were the same (the inevitable deviations had no practical meaning). Thus, the selected frequencies for all samples were in the interval $52.2 - 52.5\ Hz$. The experimental results for all groups were summarized in S-N curves, the fatigue behavior was evaluated based on test 10^6 cycles.

The failed fatigue specimens from group IV are shown in fig. 4.5.

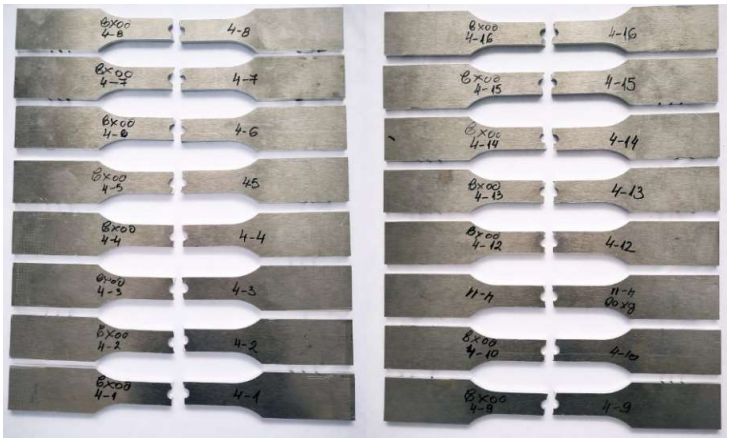

Fig. 4.5 Failed fatigue samples from group IV

4.3. Experimental results

4.3.1 $S-N$ curves

The resulting S-N curves for the four groups of experimental specimens are shown in Figure 4.6 in a double logarithmic scale. The FL of the three groups of specimens (II, III, and IV), whose holes were processed using the MSMCW method, show a significant improvement compared to the first (reference) group of specimens.

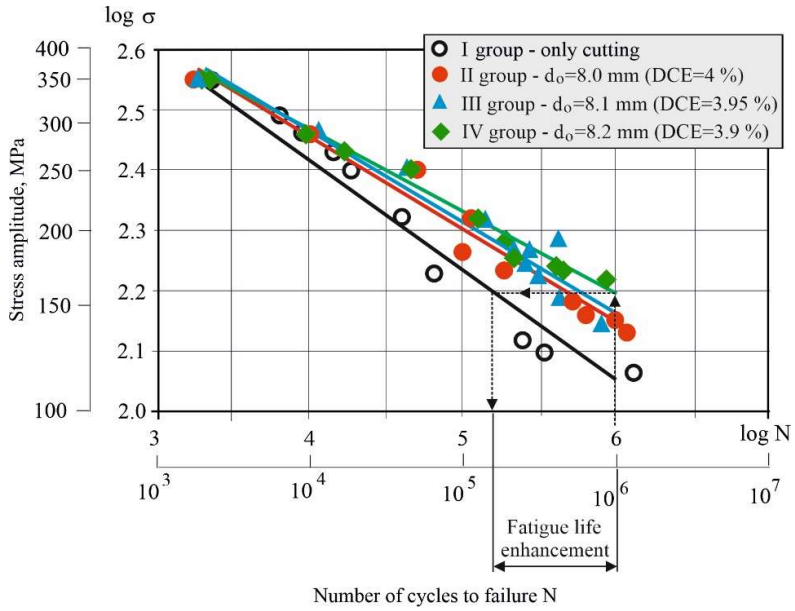

Fig. 4.6 S-N криви

The experimental samples are improved the effectiveness of MSMCW method for improving the fatigue behavior under cyclic tension of structural elements made of aluminum alloy 2024-T3.

- The S-N curves corresponding to the specimens of Groups II, III, and IV, whose holes were prestressed by the new split mandrel process, are very close to each other. This confirms the effectiveness of the new method in the conditions of excessive scattering of pre-drilled holes ($0.2\,mm$ with nominal diameter $8\,mm$);
- A slight tendency to change the slopes of the $S-N$ curves in correlation with the nominal diameter of the pre-drilled holes is observed. Although the DCE is the largest for Group II ($DCE = 4\%$), their corresponding $S-N$ curve shows a tendency toward the lowest value of 10^6 cycle fatigue strength compared to those for Groups III and IV. The greatest FL is observed in Group IV, whose pre-drilled holes have the largest nominal diameter, i.e., DCE is the smallest (3.9 %). The difference in the obtained $S-N$ curves can be explained by the difference in the introduced residual compressive circumferential stresses around the hole after cold working CEH and, above all, by the effect of redistribution of these stresses due to the removal of a plastically deformed layer of metal of different thickness after the final reaming. The appropriate thickness of the metal cut layer via the final reaming minimizes the residual stress axial gradient and, thus, homogenizes the compressive zone.

4.3.2 Repeatability of the Fatigue Behavior

To evaluate the repeatability of the fatigue behavior of specimens whose holes were prestressed using the new method, Groups II, III, and IV (20 specimens each). They were subjected to a cyclic tensile pulsation cycle with the same stress amplitude of 170 MPa until complete destruction. The number of cycles to failure was determined for each specimen.

The center of clustering was taken as the final number of cycles for each group. The results are shown in fig. 4.7.

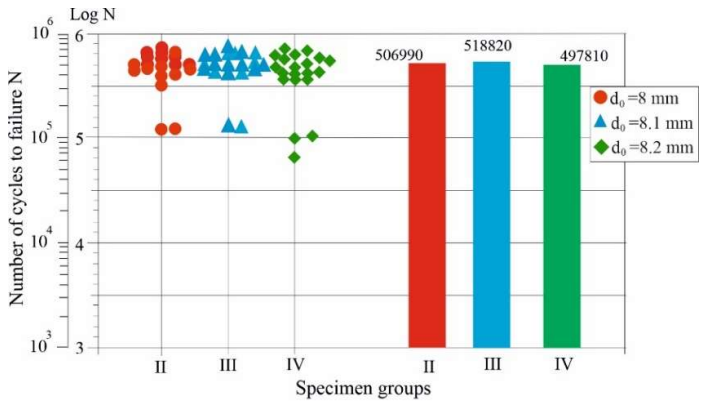

Fig. 4.7 Repeatability of the fatigue behavior.

The experiment shows that the number of cycles to failure of the three groups for a stress amplitude of 170 MPa, varies in a narrow range: from 497 810 for Group IV to 506 990 for Group III. These results confirm the observed trend for S-N curves and show that the MSMCW method provides constant fatigue strength for a given stress amplitude.

4.4. Conclusions

The results from the conducted study on the fatigue behavior of sheet specimens made of high-strength aluminum alloy 2024-T3 under a pulsating tension cycle confirm the following:

► The removal of a plastically deformed layer of suitable thickness around the hole during final reaming provides a homogenizing effect of the residual circumferential stress zone in the axial direction, which favors the improvement in fatigue behavior;

► Based on a comparative experimental study of fatigue behavior in a pulsating cycle, the effectiveness of the MSMCW method increases FL significantly – more than six times on a basis of 10^6 cycle fatigue strength compared to the conventional case of machining holes with only cutting;

► The obtained S-N curves confirm the effectiveness of the new method in the conditions of excessively large scattering (0.2 mm at a nominal diameter of 8 mm) of the pre – drilled hole diameters;

► The obtained experimental results correspond to a worst-case scenario of the diameter scattering of the pre-drilled holes. Therefore, the reductions in the dispersion of the diameters and cylindricity deviations of the pre-drilled holes are reflected in a significant increase in the efficiency of the MSMCW method.

CONTRIBUTIONS

A. Scientific and applied contributions

♦ Morphological classification scheme of the main approaches and the methods realizing them for increasing the FL of metal structural elements with FH;

♦ It has been proven that, under conditions of excessively large dispersion of the diameters of the pre-processed holes, the MSMCW method provides an intensive and deep zone with introduced beneficial hoop RSs on both end faces of sleeve-type samples made of 2024-T3 aluminum alloy after CEH and after final reaming of the holes;

♦ The effect of grain refinement near the surface of the holes in 2024-T3 aluminum alloy after CEH by the MSMCW method under conditions of different pre-processed hole diameters was established;

♦ It was found that the microhardness on the end faces of 2024-T3 aluminum alloy samples subjected to CEH with different initial hole diameters is 25 % higher compared to that in the as-received condition;

♦ Based on the microhardness profiles in axial sections, the presence of a gradient in the circumferential direction was established, due to the difference in equivalent plastic deformation in axial sections corresponding to the planes of symmetry of the segment and the notch of the tool implementing the MSMCW method;

♦ It has been proven that the removal of a plastically deformed layer of appropriate thickness around the CEH during final reaming provides a homogenizing effect in the distribution of the hoop

RSs in the axial direction, which improves the fatigue behavior under pulsating cycles of sheet components made of 2024-T3 aluminum alloy;

♦ S – N fatigue curves for pulsating cycles, proving the effectiveness of the MSMCW method under conditions of excessively large dispersion of the pre-processed hole diameters for increasing the FL of 2024-T3 aluminum alloy more than six times (based on fatigue strength at 10^6 cycles) compared to the conventional case of processing the FH;

B. Applied contributions

♦ An economically effective process for CEH, ensuring constant tightness under conditions of excessively large dispersion of the pre-processed hole diameters;

♦ A database for the characteristics of SI (RSs, microhardness, microstructure) in sleeve-type samples of 2024-T3 aluminum alloy, subjected to CE using the MSMCW method in correlation with the degree of cold expansion DCE and the thickness of the metal layer during final reaming;

♦ A database for the FL of the pulsating cycle of flat samples with FH of 2024-T3 aluminum alloy, processed only by cutting and by the MSMCW method in correlation with the degree of cold expansion DCE and the thickness of the metal layer during final reaming.

List of publications related to the dissertation

1. Anchev A.P., Dunchev V.P., **Daskalova P.H.**, Fatigue behavior experimental study of specimens with fastener holes in 2024-T3 aluminum alloy subjected to cold expansions via modified split mandrel method. International Scientific Conference, "Mechatronic, Eco – and energy saving systems and technology". Gabrovo. 2023 p.155-164 ISSN 2815-4924

2. Maximov J., Duncheva G., Anchev A., Dunchev V., **Daskalova P.**, Modified Split Mandrel Method and Equipment to Improve the Fatigue Performance of Structural Components with Fastener Holes. Metals 2024, 14, 303 doi.org/10.3390/met14030303

3. Daskalova P. Microstructure and microhardness around holes in aluminum alloy 2024-T3 subject to cold expansion by modify Split Mandrel Method. International Scientific Conference Unitech 2024, Gabrovo, Bulgaria, Vol 2 p. 36-46, 2024

4. Dunchev V.P., **Daskalova P.H.**, Experimental study of residual stresses around fastener holes in 2024-T3 aluminum alloy via modified split mandrel method. International Scientific Conference, "Mechatronic, Eco – and energy saving systems and technology". Gabrovo. 2023 p.136-151 ISSN 2815-4924

5. Duncheva G., **Daskalova P.**, Methods for increasing the fatigue life of structural components with fastener holes- state of the art. Journal of the Technical University of Gabrovo, 68 (2024) 21-36 doi.org/10.62853/JNWG1335

CITATIONS OF PUBLICATIONS RELATED TO THE DISSERTATION

Paper:

Maximov J., Duncheva G., Anchev A., Dunchev V., Daskalova P., Modified Split Mandrel Method and Equipment to Improve the Fatigue Performance of Structural Components with Fastener Holes. Metals 2024, 14, 303 doi.org/10.3390/met14030303

A citation of work:

1. Dang Z., Peng Y., Yang R., Ge D., Yan L., Gan X. Experimental study on the effect of reaming on the fatigue life of split-sleeve cold-expanded Ti–6Al–4V alloy components. International Journal of Fatigue 188 (2024) do: 10.1016/j.ijfatigue.2024.108521

2. Li C., Wang J., Yang L., Zuo Y., Zhang Q. Influence of Mandrel's Working Length on Fatigue Strengthening Effects in Open-Hole Structures through Cold Expansion. Journal of Materials Engineering and Performance (2025) doi: 10.1007/s11665-025-11072-1

3. Hossen M.S., Santana L.B., Tan H., Kim D. Finite Element Analysis to Investigate the Effects of Split Sleeve Cold Expansion Process Variables on Residual Stress Distribution and Pulling Force Progression for Al 2024-T351 Alloy. International Journal of Aerospace Engineering, (2025) (1) doi: 10.1155/ijae/6296329

4. Wan N., Zhao B., Ding W., He Q. Advancements in cold extrusion anti-fatigue manufacturing technology for connecting holes. Engineering Fracture Mechanics (2025), 314 doi: 10.1016/j.engfracmech.2024.110764

5. Wan N., Zhao B., Ding W., He Q. Research status and tendency on cold expansion anti-fatigue manufacturing technology for aircraft structural fastening holes. Journal of Manufacturing Processes (2025), 141, pp. 319 – 335 doi: 10.1016/j.jmapro.2025.02.068

6. Mu Y., Shi H., Zuo Y. Effect of Coupling Ultrasonic Fatigue Strengthening and Polishing Methods on Open Hole Structures. Journal of Materials Engineering and Performance (2025), 34 (13), pp. 13536 – 13546 doi: 10.1007/s11665-024-10125-1

7. Zhang Q., Zuo Y., Wu Q., Hu Z. Mechanical effects of interference fitting on joints with small edge distance and large pin diameter. Journal of Mechanical Science and Technology (2025), 39 (9), pp. 5037 – 5049 doi: 10.1007/s12206-025-0812-2